

Naïve to Primed Pluripotency Transition is Mediated by Primitive Ectoderm-Like Cells

Aaron Kwong

Human Genetics

McGill University, Montreal

Submitted July, 2017

A thesis submitted to McGill University in partial fulfillment of the requirements of the degree
of Master of Science

© Aaron Kwong 2017

Table of Contents

List of Tables	3
List of Figures	3
List of Abbreviations	3
Abstract	4
Resumé	6
Acknowledgments.....	8
Preface and Contribution of Authors	8
Introduction.....	9
Early Mouse Embryo Development.....	9
Naïve ESC Differentiation via EB Formation Requires FGF/ERK Signaling.....	10
ECM-Integrin Stimulates FAK Dependent ERK2 Activation	12
Intermediate Pluripotency: EB Formation and in vitro ESC Culture.....	14
Limitations in EB Differentiation of ESCs	16
Rationale and Hypothesis	18
Materials and Methods.....	19
Results.....	25
1. Rosette Organization is Associated with a Basal F-Actin Network Contractility.....	25
2. 3D Culture Directs ESCs into E5.5-like PEct Cells	33
3. FGF4 is required for naïve exit in 3D Culture.....	37
4. ECM Promotes ESC Polarization in 2D Culture without Lif+2i.....	49
Discussion.....	53
Conclusion & Future Directions	57
Appendix.....	60
Mouse Training Theory Certificate.....	60
Mouse Workshop Certificate	61
Bibliography	62

List of Tables

1. Primary Antibodies Used.....	21
2. Secondary antibodies and small organic fluorophores used.....	22
3. qRT-PCR Primers.....	23

List of Figures

Fig. 1: 3D ESC culture form polarized monolayer cysts by 72h.....	26
Fig. 2: 3D ESC culture progression from amorphous clusters to rosettes.....	30
Fig. 3: GPI::GFP rosette division at 48h.....	32
Fig. 4: qRT-PCR analysis of 3D ESC culture over 72h.....	34
Fig. 5: Inhibitor treatment of 3D ESC cultures show FGF/ERK but not Integrin/ERK dependence for naïve exit.....	39
Fig. 6: B6 <i>Fgf4</i> ^{del/del} ESC exhibit flat morphology in 2i+Lif conditions.....	42
Fig. 7: Endogenous <i>Fgf4</i> expression is critical for naïve exit and cyst formation.....	45
Fig. 8: Grb2 is critical for 3D ESC culture naïve exit and cyst formation.....	48
Fig. 9: ECM and endogenous <i>Fgf4</i> expression regulates morphology and polarization in 2D ESC culture.....	52

List of Abbreviations

Actin foci (AF), anterior visceral endoderm (AVE), disorganized cluster (DC), distal visceral endoderm (DVE), embryoid body (EB), epiblast like cell (EpiLC), primitive ectoderm like cell (EPL), embryonic stem cell derived (ESD), embryonic stem cell (ESC), organized cluster (OC), primitive ectoderm (PEct), primordial germ cell (PGC), primordial germ cell-like cell (PGCLC), primitive streak (PS), transcription factor (TF)

Abstract

Current advances in embryonic stem cell (ESC) research has successfully isolated two states of pluripotency: naïve and prime. Naïve pluripotency is considered as the ground state of pluripotency and is widely used as a tool for generating specific cell types for clinical and research applications. However, current protocols for ESC differentiation (eg. embryoid bodies) are limiting due to their efficiency. Here we describe a 3D extracellular matrix culture model for differentiating naïve ESCs into primitive ectoderm (PEct) like cells by culturing singularized naïve ESCs without 2i+Lif in 6% Matrigel suspension. 3D ESC colonies self-organize into a rosette by 48h and a monolayer cyst by 72h with luminal apical domain, similar to developmental epiblast reorganization in E4.5-5.5 embryos. qRT-qPCR analysis showed ESC in 3D culture exit naïve pluripotency with downregulated *Rex1* and *Fgf4*. PEct markers including *Otx2*, *Fgf5*, *Oct6*, *Dnmt3b*, and *Id3* were upregulated, but TGF- β factors *Nodal* and *Cripto* were not suggesting ESC in 3D culture have not entered primed pluripotency but adopt a PEct-like state. Inhibiting FGFR+MEK but not Integrin+FAK blocked naïve exit and prevented cell polarization suggesting FGF/ERK but not FAK/ERK is critical for cyst formation. *Fgf4^{del/del}* ESCs were similarly not able to exit naïve pluripotency and showed weak polarization by 72h, suggesting auto- and paracrine FGF4 is critical for naïve exit. Although FGF/ERK signaling is necessary for naïve exit, it is not clear how ECM-integrin interactions influence cyst development and cell polarization. To test this *Fgf4^{wt/wt}*, *Fgf4^{wt/del}*, and *Fgf4^{del/del}* ESC without 2i+Lif were plated on gelatin, collagen, fibronectin, laminin, or Matrigel coated glass-bottom dishes. WT-ESCs cultured on fibronectin after 72h showed the highest levels of PARD6B and aPKC enrichment, whereas gelatin and collagen showed the weakest, indicating fibronectin is a major ECM stimulant for ESC polarization upon 2i+Lif removal. These results demonstrate ESC

in 3D culture directs differentiation into PEct-like fate which is important for understanding ESC differentiation and for clinical applications.

Resumé

Les avancées actuelles dans la recherche sur les cellules souches embryonnaires (ESC) a isolé avec succès deux états de pluripotence: naïf et prime. La pluripotence naïve est considérée comme l'état fondamental de la pluripotence et est largement utilisé comme un outil pour générer des types de cellules spécifiques pour les applications cliniques et de recherche. Cependant, les protocoles actuels pour la différenciation ESC (par exemple, les corps embryoides) sont limitatifs en raison de leur efficacité. Nous décrivons ici un modèle de culture de matrice extracellulaire 3D pour différencier les ECN naïfs en cellules ectodermiques (PEct) primitives en cultivant des CES naïfs singularisés sans 2i + Lif dans 6% de suspension Matrigel. Les colonies 3D ESC s'auto-organisent en une rosette à 48h et un kyste monocouche de 72 heures avec un domaine apical luminal, Semblable à la réorganisation de l'épiblast du développement dans les embryons E4.5-5.5. L'analyse de qRT-qPCR a montré que l'ESC était dans la culture 3D de la pluripotence naïve avec Rex1 et Fgf4 à régulation négative. Les marqueurs PEct incluant Otx2, Fgf5, Oct6, Dnmt3b et Id3 ont été régulés à la hausse, mais les facteurs TGF- β Nodal et Cripto ne suggéraient pas que l'ESC en culture 3D n'ait pas entré dans la pluripotence amorcée, mais adopte un état de type PEct. L'inhibition de FGFR + MEK, mais pas la sortie naïve d'Integrin + FAK, empêchait la polarisation cellulaire suggérant FGF / ERK mais pas FAK/ERK est critique pour la formation de kyste. *Fgf4*^{del/del} ESC n'étaient même pas en mesure de sortir de la pluripotence naïve et affiché une polarisation faible de 72h, ce qui suggère que le FGF4 automatique et paracrine est essentiel pour la sortie naïve. Bien que la signalisation FGF/ERK soit nécessaire pour une sortie naïve, il n'est pas clair comment les interactions ECM-intégrine influencent le développement des kystes et la polarisation des cellules. Pour tester ce *Fgf4*^{wt/wt}, *Fgf4*^{wt/del} et *Fgf4*^{del/del} ESC sans 2i + Lif ont été plaqués sur des verres en verre à base de gélatine,

de collagène, de fibronectine, de laminine ou de Matrigel. Les WT-ESC cultivés sur la fibronectine après 72h ont montré les niveaux les plus élevés d'enrichissement PARD6B et aPKC, tandis que la gélatine et le collagène ont montré le plus faible, indiquant que la fibronectine est un stimulant ECM majeur pour la polarisation ESC lors d'une élimination 2i + Lif. Ces résultats démontrent que l'ESC dans la culture 3D oriente la différenciation en un destin de type PEct qui est important pour comprendre la différenciation ESC et pour les applications cliniques.

Acknowledgments

I would like to thank Dr. Yojiro Yamanaka for his mentoring and commitment to this research as my supervisor, as well as the editing of this thesis. I would like to acknowledge Dr. Luke McAffrey and Dr. Aimee Ryan for their thoughtful input, mentoring, and critique of my research as well as being members of my committee. I would like to thank the Canadian Institutes of Health Research (CIHR), the McGill Faculty of Medicine (Dr. Arthur H. Judson Fellowship), and the National Sciences and Engineering Research Council of Canada (NSERC) for their generous funding in this project. I would like to thank the Department of Human Genetics for tuition aid and excellence awards in my pursuit of scientific training and career development.

Preface and Contribution of Authors

I would like to thank Nobuko Honma-Yamanaka for her generous aid in the maintenance of lab mice and preparation of mice mating necessary for in-house ESC establishment, as well as previous establishment of *Fgf4* knockout mice. I would like to thank Deepak Saini for his skilled work in injecting my sgRNA into E0.5 zygotes for establishing our *Grb2* mutant line. I would like to thank Navid Nekain for his help in maintaining ESC lines used in this research as well as helping establish our *Grb2* mutant line. I would like to thank Dayana Krawchuck for her previous work in establishing a wt B6 ESC line which was used in this research.

Introduction

Early Mouse Embryo Development

Current advances in ESC research has successfully isolated two states of pluripotency: naïve and prime. Naïve pluripotency is considered as the ground state of pluripotency with its developmental analog most similar to the epiblast of E4.5 mouse embryos ¹. Primed pluripotency is a differentiated cell type to naïve and is most developmentally similar to the anterior primitive streak (PS) of E6.5 mouse embryos ². Compared to naïve, primed pluripotent cells have a hypermethylated genome ³⁻⁵, inactivated x-chromosome ⁶, and cell polarity ⁷. Nonetheless, primed pluripotency retains functional pluripotency with its ability to form chimeras when developmentally matched embryos are used as hosts (eg. E6.5-E7.5 epiblast, but not E8.5) ^{8,9}. However, new evidence suggests ~E5.5 epiblast cells are distinctly separate from naïve or primed ESC, but instead are an intermediate form of pluripotency ^{10,11}.

During the peri-implantation stage (E4.5-E5.5), the epiblast cells within the implanting embryo reorganize into a rosette and expand into a monolayer cyst ¹². Reorganization into a rosette is associated with gain of cell polarity around late E4.5-E4.75 as indicated by enriched aPKC at the rosette center prior to lumen formation. Cavitation of the rosette to form a monolayer cyst has been attributed to the localization of podocalyxin at the apical domain of ESCs ¹³ and MDCK cells ¹⁴ in 3D culture. This negatively charged membrane protein has been shown to have anti-adhesion properties for lumen formation in MDCK cells ¹⁵. Shortly after epiblast lumen formation (E5.25), extra-embryonic ectoderm also begins lumen formation which coalesces with the epiblast lumen by E5.75 ¹². The resulting embryo forms a continuous monolayer epithelium consisting of proximal extra-embryonic cells and distal epiblast cells with

a single amniotic cavity (egg cylinder cone). At this point, the epiblast cells are commonly referred to as PEct.

PEct cells are highly competent to receive signals for differentiation. Posterior PEct cells are developmentally fated for the primitive streak (PS). PEct cells secrete an immature form of Nodal—a transforming growth factor β (TGF- β) secreted ligand—which is cleaved into a mature form by an extra-embryonic secreted protease, furin for autocrine activation of Nodal signaling leading to PS formation. Nodal signaling activation is limited to the posterior PEct due to proximal-distal and anterior-posterior signaling gradients. Secretion of Nodal antagonists like Cer1 and Lefty1/2 from the distal visceral endoderm (DVE) prevents the activation of Nodal signaling of nearby epiblast cells. Anterior migration of the DVE to form the anterior VE (AVE) further blocks the activation of nodal signaling in the anterior PEct, thus establishing the anterior-posterior axis along the gradient of Nodal signaling and limiting PS formation to the posterior. PS formation is enhanced through canonical Wnt signaling via Wnt3 secretions from the posterior VE ¹⁶. Wnt signaling at the posterior PEct promotes the transcription factor (TF) activity of β -catenin to bind to the proximal epiblast enhancer of *Nodal* to increase its expression and subsequent positive feedback of the Nodal-FoxH1 autoregulatory loop which further increases Nodal expression in the PS ^{17,18}. *Wnt3* expression in the posterior VE is not essential for initiating PS formation, as *Wnt3*^{-/-} VE only delays PS formation ¹⁹. However, Wnt signaling does promote *T* expression which is a pan mesodermal marker, essential for mesoderm formation and PS development ²⁰. Indeed, Wnt signaling within the PEct is context dependent as it promotes both neural crest and PS formation depending on Nodal signaling activity ^{16,19}.

Naïve ESC Differentiation via EB Formation Requires FGF/ERK Signaling

Although naïve embryonic stem cells (ESCs) have the capacity to differentiate into all three germ layers and their respective cell lineages, they are not readily competent for *in vitro* differentiation. In order to initiate differentiation, formation of embryoid bodies (EB) is required^{21–24}. EBs are spheroid aggregates of ESCs, usually naïve mESC or primed hESC, that are cultured in suspension to allow ESCs establish competency for differentiation. EB formation from mouse naïve ESCs is dependent on FGF/ERK and PI3K-AKT signaling pathways^{25–27}. Blocking the FGF signaling by overexpression of a dominant negative form FGFR2 which has been suggested to block FGFR1/2/3/4 activity through heterodimer inactivation, can prevent to form EBs with internal epithelial cysts, a morphological landmark for proper EB formation²⁵. Similarly, *Grb2*^{-/-} ESCs—the gene encoding an adapter protein critical for FGF/ERK signal transduction—failed to form cavitated EBs and did not yield visceral endoderm colonies from EB differentiation^{28,29}. Additionally, *Ext1*^{-/-} ESCs—the gene encoding an enzyme that polymerizes heparin (Hep) sulfate precursor structure which regulates FGF ligand-receptor binding—failed to form cavitated EBs and showed no upregulation in early endoderm, mesoderm, and extraembryonic tissues specific markers³⁰. While FGF/ERK signaling is critical for ESC multilineage differentiation in EBs, it also is a key regulator in EB-free differentiation. ESCs in N2B27 media normally differentiate into neural Tuj1+, Oct4- cells in *in vitro* 2D culture without LIF. However, the majority of *Fgf4*^{-/-} ESCs fail to form neural cells with minor sporadic exceptions³¹. Similarly, the majority of *Fgfr1*^{-/-} ESC are not able to differentiate into Tuj1+ neural cells in N2B27 media, or Gata4+ PE cells in trophoblast stem (TS) cell media with supplemented FGF2+Hep+retinoic acid+activin A³². Interestingly, *Fgfr2*^{-/-} ESCs are still able to differentiate into Gata4+ PE cells, highlighting the importance of *Fgfr1* over *Fgfr2* in FGF/ERK stimulated ESC differentiation. Similar to EB dependence on FGF/ERK signaling for

differentiation, *Fgf4* null embryos quickly leads to embryo degeneration with either a small disorganized or undetectable PEct layer by E6.5³³, suggesting FGF/ERK signaling is critical during implantation.

Although FGF/ERK signaling is critical for naïve ESC differentiation, FGF/ERK signaling in EpiSCs is critical for maintaining self-renewal capacity³⁴. EpiSCs is cultured in the presence of MEK inhibitor PD0325981 or without exogenous FGF2 demonstrate downregulation of the pluripotency factors *Oct4* and *Nanog*. EpiSCs in this condition also show an upregulation of *Otx2* which subsequently induces *Pax6* expression, specifying neurectoderm differentiation³⁵. Indeed, FGF/ERK signaling blocks neurectodermal differentiation in EpiSCs. However, EpiSCs can be maintained in culture without exogenous FGF2 if Nodal signaling is highly activated.

ECM-Integrin Stimulates FAK Dependent ERK2 Activation

While the FGF/ERK pathway is most commonly attributed to stimulating naïve ESC differentiation and EB formation, integrins have also been demonstrated to upregulate ERK signaling. Integrins are membrane proteins that directly bind to extra-cellular matrix (ECM) proteins (eg. Fibronectin, and laminin) to signal environmental niche conditions to the cell. Integrins have no catalytic activity unlike FGFR, which is a tyrosine kinase receptor. Instead, integrin α and β monomers form a heterodimer and bind to a specific ECM protein to form focal adhesion sites (FAS)^{36,37}. Once integrin-ECM complexes are formed, they recruit additional structural and enzymatic proteins including focal adhesion kinase (FAK), c-Src, Shc, and Grb2^{38,39}. FAK is a critical tyrosine kinase that regulates cell survival, cytoskeletal dynamics, cell motility, and ras activation^{40,41}. RAS is an upstream GTPase that is responsible for ERK1/2 phosphorylation for activated ERK signaling. While the exact mechanism has not been fully elucidated, FAK seems to form a dynamic and complex with GRB2, c-SRC, and SHC2 for

subsequent Ras activation³⁹. FAK recruited to FASs is quickly autophosphorylated at Tyr-397. pTyr-397 FAK then acts as a kinase and phosphorylates c-Src for activation. Together activated FAK and c-SRC targets SHC2 for phosphorylation which allows it to complex with GRB2 for SOS dependent Ras activation⁴². GRB2 is an adapter protein that is critical for FGF/ERK activation by binding FRS2—an adapter protein that directly binds to activated FGFR—and SOS—a guanine exchange factor—for downstream RAS activation. SHC2 is also an adapter protein that binds to activated FGFR and GRB2 for downstream RAS activation, however it has been implicated as a direct antagonist with FRS⁴³.

Plating NIH3T3 fibroblasts on fibronectin coated dishes has been shown to activate $\alpha_5\beta_1$ -integrin FAS for FAK phosphorylation at Tyr-397, and subsequent downstream Ras activation^{39,41,44}. Overexpressing a dominant negative Phe-397 FAK in fibronectin stimulated NIH3T3 fibroblasts has been demonstrated to block ERK2 phosphorylation to levels similar to dominant negative Asn-17 Ras, suggesting FAK phosphorylation at Tyr-397 is critical for Ras activation⁴⁴. Indeed pTyr-397 FAK is necessary for c-Src binding and phosphorylation. Although FAK can bind to Grb2 directly if phosphorylated at Tyr-925, mutant Phe-925 FAK expressed in fibronectin stimulated fibroblasts show increased Erk2 phosphorylation. This suggests FAK-GRB2 complex is not necessary for ECM/Ras activation. However, chemical inhibition of FAK using cytochalasin D which blocks actin polymerization, was sufficient to block FAK phosphorylation but still retain c-SRC and ERK2 phosphorylation⁴⁵. While cytochalasin D does not block FAK recruitment to the membrane in fibronectin stimulated fibroblasts, these results suggest FAK acts as an important structural protein and kinase for ECM dependent Ras activation³⁹.

Intermediate Pluripotency: EB Formation and in vitro ESC Culture

EB development has been shown to correlate well with peri-implanted embryos both in gene expression and morphology. EBs at 48h have been shown to retain *Oct4* expression—a key pluripotency TF—whilst having downregulated *Rex1* and *Fgf4*—markers for naïve pluripotency—suggesting ESCs have exited naïve pluripotency. Interestingly, EBs at this stage have upregulated *Fgf5* but not *T* expression, both primed pluripotency markers⁴⁶. This early expression pattern is concatenate with E5.5-5.75 epiblast cells which are *Oct4+*, *Fgf5+*, *Rex1-*, and *T-*^{1,47,48}. EB development mimics peri-implantation epiblast development by developing multiple cysts per EBs after 4-5 days in culture^{22,49}. ECM-Integrin interaction has also been shown to be necessary for cortical PE formation in EBs. Mature EBs form a cortical monolayer of primitive endoderm cells surrounding epithelial cysts. Interestingly, *Itgb1* null EBs fail to form a proper cortical layer of GATA4+ cells, indicating primitive endoderm cells, and fail to form inner cysts⁵⁰. Similarly, *Itgb1* null embryos have disrupted epiblast-primitive endoderm segregation in peri-implanted E4.5 and E5.5 embryos^{51,52}. 3D Matrigel *in vitro* culture of ESC has been shown to reorganize into a monolayer cyst resembling the developing PEct with luminal apical domains¹². However, *Itgb1* null ESCs fail to self-organize into a monolayer cyst and instead form amorphous cell aggregates with some cells carrying apical domains.

Primitive ectoderm-like cells (EPL) from naïve ESCs *in vitro* have been previously isolated using 50% supplemented HepG2 conditioned media⁵³. The EPL cells are *Fgf5+*, *Rex1-*, and *Gbx2-* which is a naïve ESC marker whilst still retaining *Oct4* expression. In this culture condition, they form flat epithelial like colonies similar to EpiSC and can be passaged >40x without differentiating into neural lineages, demonstrating their high capacity for self-renewal. This is however dependent on HepG2 conditioned media supplementation. EPL colony

formation is optimal when plated on collagen IV and fibronectin ⁵⁴. Interestingly, EPL cells can be derived from E5.5 but not E6.5 or E7.5 mouse embryos ⁵⁴. This time frame of EPL isolation is particularly narrow compared to ESC which can be isolated at E3.5-4.5 (pre-implantation), and EpiSC which can be isolated from embryos E5.5-6.5 ⁵⁵. Although key differentiation factors in the HepG2 conditioned media has been analyzed ⁵⁶⁻⁵⁹, no clear factor has been linked to maintaining EPL cells. It is noteworthy that ECM proteins including fibronectin 1, fibrinogen alpha chain, and fibrinogen gamma polypeptide have been identified in HepG2 conditioned media ⁵⁹, as it has been demonstrated that EPL colony formation is ECM sensitive, suggesting ECM-integrin signaling is important for EPL maintenance ⁵⁴. Although EPL cells show gene expression markers similar to peri-implanted embryos, EPL cells are not able to form chimeras when introduced into donor blastocysts ⁵³. Contrastingly, E5.0 epiblast cells are able to form chimeras when introduced into a donor blastocyst ⁶⁰, suggesting EPL are not functionally analogous to peri-implanted epiblast cells (E4.75-5.5).

Epiblast-like cells (EpiLC) are 2D naïve ESC cultures with supplemented bFGF+activin A, two factors critical for EpiSC differentiation and maintenance ^{34,55}, that exhibit PEct-like gene expression patterns ^{3,61-63}. EpiLC show downregulated naïve factors over 72h including *Nanog*, *Prdm14*, *Rex1*, *Tbx3*, *Klf2*, *Klf4* and upregulated primed factors including *Fgf5*, *Dnmt3b* ^{61,62}. However, EpiLC are a transient state of ESC since after 72h significant cell death is observed. Primordial germ cells (PGC) arise from the E6.0 proximal egg-cylinder cone due to Bmp4 stimulation from the extraembryonic ectoderm ⁶⁴. FACS analysis of EpiSC in typical bFGF+activin A media showed a small population of Stella-GFP+ cells (~1.5%), a marker for early PGCs, suggesting a subset of cells in EpiSC culture are PGC-like cells (PGCLC) *in vitro* without exogenous Bmp4 ⁶⁵. However, direct differentiation of EpiSC into PGC-like cells

(PGCLC) by culturing with supplemented Bmp4 over 72h only increased Stella-GFP+ cell count to 2.3%, suggesting EpiSC are not competent to differentiate into PGCLC from Bmp4 stimulation. Since *in vivo* PGCs derive from the PEct, it is expected that EpiLC would be better suited to differentiate into PGCLC over EpiSC due to their more primitive pluripotency state and PEct-like epigenetics³. Indeed, culturing EpiLC in suspension with supplemented Bmp4/8b+SCF+LIF+EGF (SCF: stem cell factor; EGF: epidermal growth factor) yields 7.2% Blimp1+ Stella+ cells⁶¹. Introduction of these cells into mouse testes lacking endogenous spermatogenesis was able to successfully rescue functional spermatozoa production and yield healthy offspring. These results suggest EpiLC exhibit functional and epigenetic qualities similar to E5.5 PEct.

Limitations in EB Differentiation of ESCs

Although EB formation is a commonly used strategy for initial ESC differentiation, it suffers from two limitations, which prevent it from being a gold standard of ESC differentiation. Firstly, efficiency of EB differentiation is size dependent. EBs formed within the same culture come in a range of varied sizes which effect their differentiation potential. EBs that are too small fail to differentiate, while EBs that are too large develop necrotic centers which has been linked with nutrient and cytokine diffusion limitations^{23,66}. Microfabricated devices which have pores for EB trapping have been developed for EB size screening to mitigate this limitation^{23,67}. Secondly, EB formation is not efficient to generate specific lineages due to their heterogeneous composition^{21,68}. It is unclear whether this heterogeneity is due to spontaneous or instructed differentiation cues via secreted morphogens, ECM, or cell-cell contact stimulation. Regardless, every EB contains cell types within all three germ layers thus limiting their potential for homogenous directed ESC differentiation.

EB-free cell differentiation protocols offer the potential for homogeneous ESC differentiation, but are typically severely limited in their efficiency. Culturing ESCs in the presence of stromal cells can support hematopoietic differentiation. Differentiation is sporadic with very low efficiency (<1% differentiation) and is dependent on the stromal cell line and passage number of ESCs ^{69,70}. Secreted factors from the stromal cells necessary for hematopoietic differentiation are not well defined and thus have not yet been adopted for minimal media differentiation protocols. Culturing monolayer ESCs in defined media on ECM coated dishes promotes neurectoderm differentiation ^{71,72}. Neurectoderm differentiation is one of the few protocols where homogenous and efficient ESC differentiation can be accomplished in *in vitro* 2D culture. However, neurectoderm differentiation is often seen as the ‘default’ path of ESC differentiation in the absence of other morphogens and is not applicable for other differentiation lineages ⁷³. Non-EB differentiation protocols are not generalizable and practical for most ESC differentiation lineages due to their extremely low efficiency rates ^{21,23}. An isolated form of ESCs competent for differentiation is necessary for efficient, defined, *in vitro* directed differentiation.

Rationale and Hypothesis

It has been demonstrated that ESCs in 3D culture develop into monolayer cysts which morphologically resemble E4.5-5.5 epiblast development ¹². Although these cells have not been confirmed to be PEct-like functionally or transcriptionally, they exhibit similar morphological development to EBs which have been shown to have peri-implanted embryo gene expression patterns ^{1,25,46-48,50}. Since morphology and cell state are highly linked, this suggests that ESC in 3D culture have exited from naïve pluripotency and adopted peri-implantation epiblast-like qualities. **I hypothesize that that 3D culturing ESCs directs differentiation into PEct-like cells, similar to early EB formation.**

Materials and Methods

Naïve ESC Culture. ESCs were derived in house by harvesting E3.5 blastocysts and incubating in KSOM for 24h at 37°C with 5.5% CO₂. Blastocysts were then cultured on gelatin coated, fibroblast plated 4-well plates for 10-14 days to form outgrowths in ES-DMEM media. Outgrowths were washed with PBS, treated with 100µL accutase (ThermoFisher) for 3min, gently pipetted to singularize, and transferred into a 35mm gelatin coated dish with 100µL ES-grade FBS (Wisent). Media was changed every 2 days and expanded by dissociated with 500µL 0.05% Trypsin-EDTA, diluted with 3-5mL of DMEM (Wisent), centrifuged for 3min at 123g, then replated in ES-DMEM onto a larger plate. ES-DMEM media contained DMEM (Millipore), 1X Sodium Pyruvate (Gibco), 1X Non-Essential Amino Acids (Gibco), 1X Glutamax (Gibco), 1X Penicillin/Streptomycin (StemCell Technologies), 0.11mM 2-mercaptoethanol (Sigma) diluted in D-PBS (MultiCell), 10% v/v Knockout Serum Replacement (GIBCO), 1µM PD0325981 (Biovision), 1µM CHIR9901 (Stemgent), and 1000U/mL Lif (Millipore). FGF4 (R&D Systems) and Heparin (R&D Systems) were supplemented accordingly.

3D ESC Culture. Naïve ESCs were cultured to ~80% confluency, washed twice with 1X PBS (MultiCell), and treated with 0.05% or 0.25% trypsin-EDTA for 3 minutes then gently pipetted to singularize. Cells were washed once with DMEM (Millipore) before diluting to the appropriate cell density with additional DMEM. Cells were pre-mixed with ice cold 3D-DMEM containing DMEM (Millipore), 1X Sodium Pyruvate (Gibco), 1X Non-Essential Amino Acids (Gibco), 1X Glutamax (Gibco), 1X Penicillin/Streptomycin (StemCell Technologies), 0.11mM 2-mercaptoethanol (Sigma) diluted in D-PBS (MultiCell), 5% v/v ES-FBS (Wisent), and 6% v/v Geltrex (ThermoFisher). Cells were plated on Poly-2-hydroxyethyl methacrylate (Sigma) coated 24-well plates at 5×10^4 cells/well. Cells were cultured at 37°C and 5.5% CO₂. PD0325981,

PD173074 (Stemgent), RGDS peptide (R&D Systems), PND-1186 (Cederlane), and DMSO (Sigma) were supplemented accordingly.

ESC-derived EpiSC Culture. ESC-derived (ESD) EpiSC were established using embryoid body culture protocol ⁴⁶. Briefly, 5×10^4 singularized naïve ESC were plated on 100mm bacterial-grade dishes in EB differentiation media. EBs were cultured for 2 days then dissociated in 0.05% Trypsin-EDTA for 3min at 37°C. Cells were washed twice with CDM then cultured at 37°C on a FBS-coated 100mm dish in CDM to establish ESD-EpiSC colonies. FBS-coated plates were produced by adding 6mL of Hi-FBS (Gibco) to a 100mm plate and incubating at 37°C overnight; plates were washed twice with 1X PBS prior to use. EB differentiation media: DMEM (Millipore), 8% knockout serum replacement, 2mM glutamine, 1mM sodium pyruvate, 0.1mM non-essential amino acids, and 0.1mM β -mercaptoethanol. CDM: 50% IMDM (Gibco), 50% F12 Nut-Mix (Gibco), 1 μ g/mL insulin (Roche), 15 μ g/mL transferrin (Roche), 450 μ M monothioglycerol (Sigma), and 5mg/mL bovine serum albumin fraction V (Sigma).

***Grb2* mutant ESC.** Male 129 wt mice were crossed with female CD1 ROSA^{Cas9/Cas9} mice. Zygotes were harvested at E0.5 and injected with sgRNA carrying 5'-CAAAGGGGGGACATCCTTA-3' sequence targeting Exon 3/protein coding region 1 of *Grb2* gene. sgRNA was produced by cloning the target sequence into pX330 plasmid carrying Cas9 scaffold protein. The DNA template was PCR amplified using the forward primer 5'-TAATACGACTCACTATAGGGCAAAGGGGGGACATCCTTA-3' carrying a 5' T7 promoter region followed by GG for enhanced transcription and the reverse primer 5'-AAAAGCACCGACTCGGTGCC-3'. Amplicon was purified using QIAEX II Gel Extraction Kit (Qiagen) and transcribed using Maxiscript T7 Kit (Ambion). Embryos were cultured in

KSOM for five days then transferred onto MEF coated 4-well plates (Nunc) for outgrowth formation and ESC derivation as per protocol described above.

3D Culture Immunostaining and Live Imaging. To ensure low optical distance of rosettes and cysts to the microscope objective lens, naïve ESC were dissociated and diluted to 8400cells/10 μ L. 10 μ L of the solution was gently dispensed in the center of 100% geltrex coated glass-bottom dish (MatTek). Ice cold 3D-DMEM was gently added to the side of the dish to avoid disturbing cell positioning proximal to the glass. Cells were cultured normally thereafter and fixed using the adapted protocol ⁷⁴. Briefly, cells were gently washed 3x with D-PBS then fixed with 4% PFA (PolySciences) or 10% TCA for 30 minutes. Cells were washed 3x with D-PBS and then 3 more times with 10min incubations at room temperature (RT) per wash. Permeabilization solution containing PBS, 0.5% Triton-X, and 10% Hi-FBS (Gibco). Cells were then stained with primary antibodies overnight followed by 3x washes with D-PBS and then 3 more times with 10min incubations at RT per wash. Cells were fixed with secondary antibodies for 3 hours at RT with shaking followed by another round of aggressive washes.

Alternatively, 3D ESC cysts were cultured as per normal in polyHEMA coated dishes and picked up using glass pipettes, washed in D-PBS with 10% fetal calf serum, then fixed in 4% PFA solution for 30min. Clusters were immunostained as described above.

Primary antibodies used:

Protein Target	Company	Reference Code
p120-catenin	BD Bioscience	610133
aPKC	Santa Cruz	sc-017781 (H1)
Claudin	Invitrogen	519000

B-catenin	Cell Signaling	L54E2
Non-phosphorylated β -catenin	Cell Signaling	S8145
E-cadherin	Life Technology	334000
Lam β 2/ γ 1	Invitrogen	MA5-14649
MLC2	Cell Signaling	3672P
pMLC2 Ser19	Cell Signaling	3671P
PARD6B	Santa Cruz	sc-37393 (M-64)
ZO-1	Invitrogen	901200

Secondary antibodies and small organic fluorophores used:

Name	Company	Reference Code
AlexaFluor 488 Phalloidin	Life Technology	A12379
Dylight 549 α -rabbit		
Dylight 649 α -mouse		715-495-151
Popo-1 DNA Stain	Invitrogen	1112977

2D ESC culture. ECM coated plates were made by incubating 200 μ L of either 1% gelatin solution (Millipore), 150mg/mL collagen from bovine skin (Sigma), 20 μ g/mL fibronectin from human plasma (Sigma), 0.5 μ g/cm² iMatrix-511 laminin fragments (Nippi), or 6% Geltrex in a well of a 8-well glass bottom slide (ibidi) overnight at 4°C. Media was aspirated prior to use. 5x10⁴ cells in 3D-DMEM without supplemented Matrigel. Cells were cultured for 72h at 37°C with 5.5% CO₂.

RT-qPCR. After mRNAs were extracted using FavorPrep Blood/Cultured Cell Total RNA Mini-kit (Favorgen), RNA was reverse transcribed via iScript cDNA Synthesis kit (BioRad) as per protocol. cDNA was diluted 1:64 or 1:4 in RNase-free water and quantified with SsoAdvanced Universal SYBR Green Supermix (BioRad) in 10 μ L reactions as per protocol. Heat steps were optimized for single peak amplicons using the following heat steps: initial denature at 95°C for 30 seconds, denature at 95°C for 10 seconds, anneal/amplify at 60°C for 20 seconds, repeat 60x, and complete with melting curve step. All genes quantified were referenced to SDHA to control for variable gene expression during ESC differentiation ⁷⁵.

qRT-PCR Primers

Gene	For Primer (5'→3')	Rev Primer (5'→3')	Source
Atp5b	AGGGGCACCAATCAAATTC	GCAGATCCACAACCTTTATCCCA	Primerbank 133892441c3
Bmp4	TGTGAGGAGTTCCATCACGA	CAGGAACCATTTCTGCTGGGG	Primerbank 121949822c3
Brachyury (T)	ACAACCACCGCTGGAAATATG	CTCTCACGATGTGAATCCGAG	Primerbank 118130357c2
Cripto	CTGCCCAAGAAGTGTTCCCTG	TCGTACAGACGGCGTTTG	Primerbank 134053944c3
Dmmt3b	GCCCATGCAATGATCTCTCT	CCAGAAGAATGGACGGTTGT	Wysocka et al. ³
FGF4	TGGGCCTCAAAGGCTTCG	CGTCGGTAAAGAAAGGCACAC	Primerbank 158508679c1
FGF5	AACTCCATGCAAGTGCCAAAT	CGGACGCATAGGTATTATAGCTG	Primerbank

			145966820c3
Id3	CTGTCGGAACGTAGCCTGG	GTGGTTCATGTCGTCCAAGAG	Primerbank 162417969c1
Lin28a	GGCATCTGTAAGTGGTTCAACG	GCCAGTGACACGGATGGATT	Primerbank 22003877c1
Lin28b	TAGGTGGAGACGGCAGGATTT	ACCACAGTTGTAGCATCTTGGA	Primerbank 294997237c2
Nanog	ATGCCTGCAGTTTTTCATCC	GAGGCAGGTCTTCAGAGGAA	Yamanaka Lab
Nodal	TCAAGCCTGTTGGGCTCTACT	GTCAAACGTGAAAGTCCAGTTCT	Primerbank 218156276c1
Nr0b1	GCGGTCCAGGCCATCAAGAGT	TCCGGATGTGCTCAGTAAGGATCTG	RT Primer DB 3946
Oct4	CACCATCTGTCGCTTCGAGG	AGGGTCTCCGATTTGCATATCT	Primerbank 356995852c2
Oct6	TCGAGGTGGGTGTCAAAGG	GGCGCATAAACGTCGTCCA	Primerbank 7106383a1
Otx2	CCACTTCGGGTATGGACTTG	GTCCTCTCCCTTCGCTGTTT	Wysocka et al. ³
SDHA	GCTCCTGCCTCTGTGGTTGA	AGCAACACCGATGAGCCTG	Golding et al. ⁷⁵
Sox1	AGACAGCGTGCCTTTGATTT	TGGGATAAGACCTGGGTGAG	Trott et al. ⁷⁶
Zfp42 (Rex1)	CCCTCGACAGACTGACCCTAA	TCGGGGCTAATCTCACTTTCAT	Primerbank 7110739a1

Results

1. Rosette Organization is Associated with a Basal F-Actin Network Contractility

Mouse naive ESCs can form monolayer cysts in 3D culture using matrigel¹². To validate our 3D culturing system, we seeded single 129 wt ESCs grown in 2i+Lif 2D culture into the 3D culture condition. Singularized ESCs in 3D culture proliferated and formed small cell clusters by 24h (Fig. 1A). These ESC clusters showed no apparent organization and were classified as amorphous aggregates. By 48h, the clusters self-organized into a rosette, which were cells in the clusters arranged in a radial pattern with high cortical roundness, but did not have a central lumen. By 72h, the rosettes formed enclosed monolayer cysts with a single clear central lumen.

To determine the onset of rosette and cyst formation of ESCs in 3D culture, we compared morphology of the cluster at 36h, 48h, and 60h after the beginning of 3D culture. The clusters were classified into 6 cluster morphology types according to distributions of nuclei in a cluster and F-actin staining patterns. First, the clusters were classified as either ‘organized’ or ‘disorganized’, where organized clusters (OC) demonstrated annular alignment of cluster nuclei as a marker for rosette organization (Fig. 1C) while disorganized clusters (DC) exhibited no annular nuclear alignment and more closely resembled amorphous cell aggregates. Both the OCs and the DCs were found with or without a central F-actin foci (AF), or lumen. The AF in OCs consistently localized at the center of the nuclear annulus, whereas the AFs in DCs localized sub-cortically but no correlation is found to nuclear position patterns (Fig. 2B). The number of cells in the clusters were also used for classification: single cell, <4cell clusters, and superclusters (2+ clusters merging).

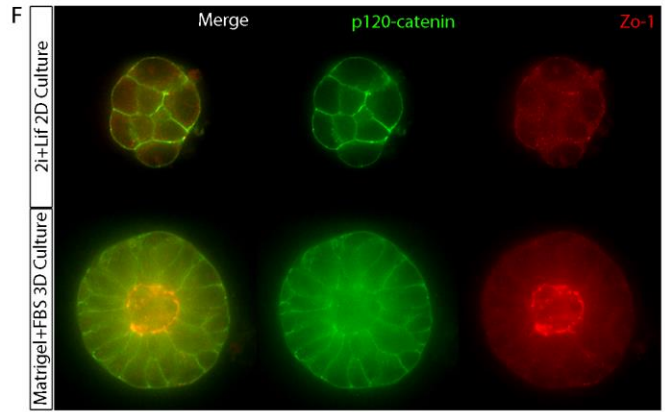
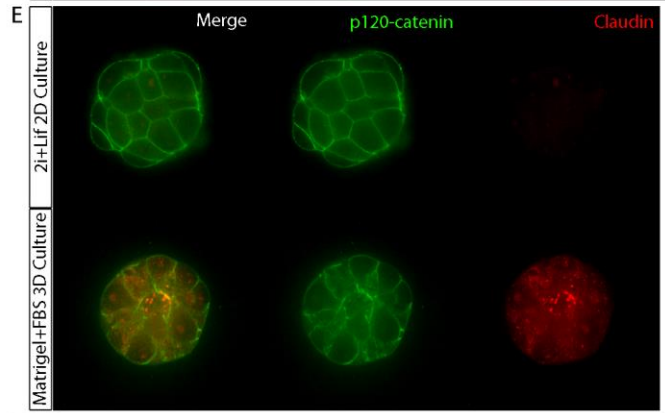
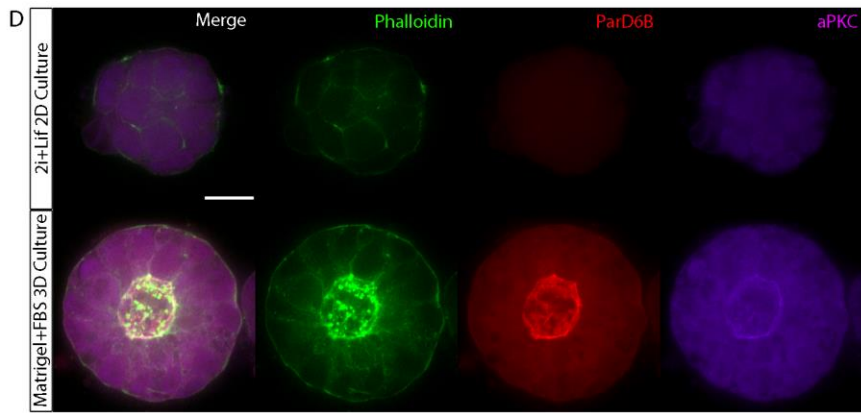
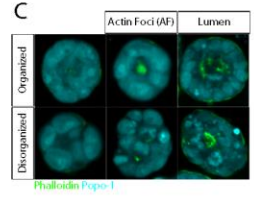
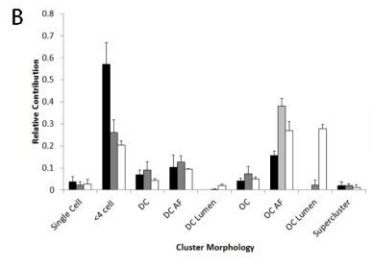
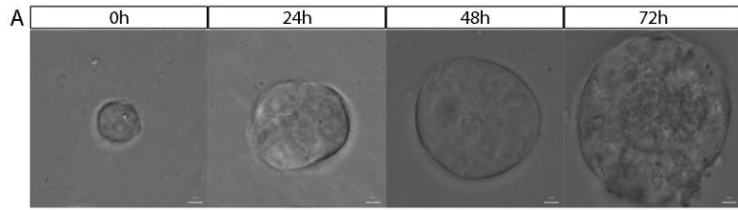


Fig. 1: 3D ESC culture form polarized monolayer cysts by 72h. 3D ESC culture from single cells (0h), form amorphous aggregates (24h), then rosettes (48h), followed by monolayer cysts (72h) (A). 72h 3D ESC cysts show enriched PARD6B and aPKC at luminal cell membrane compared to 2D ESC culture on gelatin in the presence of 2i+Lif which showed no significant enrichment (B). 3D ESC cysts show enrichment of Claudin (C) and ZO-1 (D) at apical cell-cell junctions compared to 2D ESC culture with 2i+Lif which demonstrated no significant enrichment. Scale bar set at 20 μ m.

The proportion of <4 cell aggregate population showed a strong decrease with time (0.57 ± 0.09 36h to 0.20 ± 0.02 60h) (Fig. 1B) suggesting the cluster can keep proliferating in 3D condition. The proportion of the OC-AF population showed an initial increase from 36h to 48h but then a decrease at 72h (0.16 ± 0.02 , 0.38 ± 0.03 , 0.27 ± 0.04 respectively). Interestingly this decrease appeared to correlate with a significant increase in the proportion of the OC-lumen population at 72h (0.28 ± 0.02), suggesting that the OC-AF population develops into the OC-lumen population between 48h-60h. The proportions of single cells, DC, DC AF, DC Lumen, and superclusters remained relatively low (less than 10%) across all time points (Fig. 2A), suggesting ESC in 3D culture preferably self-organize into OC-AF and OC lumen.

ESCs in 3D culture can develop to polarized monolayer cysts with luminal membrane enrichment of apical associated proteins, including aPKC¹². In order to determine if ESCs in 3D culture polarize, we examined subcellular localization of PARD6B and aPKC in the ESC derived cysts at 72hr and the ESC colonies cultured on the traditional gelatin coated 2D plastic dish for 72h in the presence of 2i+Lif (Refer to Fig. 8 for 2D culture without 2i+Lif). The Par3/Par6/aPKC complex is an evolutionarily conserved protein complex and a key regulator in polarity formation in *C. elegans*^{77,78}. Since naïve pluripotency is tightly linked with a non-polar

morphology that forms domed colonies in 2D culture ^{79,80}, we expected no enrichment for these polarity associated proteins in 2D culture. Indeed, immunostaining for PARD6B and aPKC showed that ESCs on gelatin in the presence of 2i+LIF showed no membrane enrichment of PARD6B and aPKC, but instead an even cytoplasmic staining as expected of naïve ESCs (Fig. 1D). However, in the ESCs in 3D culture after 72hrs, PARD6B and aPKC were enriched at apical luminal membranes (Fig. 1B). Claudin1 and ZO-1 are tight junction associated proteins ^{81,82}. No enrichment of these tight junction associated proteins was observed in naïve ESC cultured in 2i+Lif, while the cells in the 3D cysts showed clear enrichment at the apical cell-cell junctions (Fig. 1E+F), indicating the tight junction formation in the cysts. This suggests that non-polarized naïve ESCs acquire apico-basal cell polarity in the 3D culture condition to form epithelial monolayer cysts by 72 hr.

To characterize the onset of polarization in the 129wt ESCs in 3D culture, we examined localization of PARD6B and E-cadherin at 24h, 36h, and 48h. A previous study showed enriched aPKC at central foci within 24h of culture ¹², suggesting the formation of the apical domain in the cysts ⁷⁷. Interestingly, no PARD6B enrichment at central foci was observed in our clusters at 24h and 36h, while all clusters sampled at 48h showed ParD6B enrichment in central foci (Fig. 2A). Although no aPKC data staining data was collected during this timepoint, this difference in polarization timing may be due to difference in quality and quantity of FCS and Matrigel used (15% FCS vs 5% demonstrated here; unreported amount of Matrigel vs 6% demonstrated here), ESC strain differences (C57Bl6 vs 129 wt), or recruitment timing of Par proteins to apical domains ¹³. E-cadherin, a Ca²⁺ dependent cell adhesion molecule, localizes along lateral junctions with strong enrichment at adherens junctions in polarized cells ^{12,83,84}. Indeed, E-cadherin was enriched along lateral junctions as expected of polarized cells.

Interestingly, we also observed non-junctional enrichment of E-cadherin in cytosolic regions proximal to the apical domain. In order to verify E-cadherin was localized at cell-cell junctions and cytosolic regions, we stained with the antibody against non-phosphorylated form of β -catenin, which is sequestered to the plasma membrane for maintaining cell-cell junction integrity via cadherin/catenin complex or enriched within the nucleus for activated Wnt/ β -catenin pathway^{80,83,84}. Indeed, non-phosphorylated β -catenin and E-cadherin staining co-localized at lateral junctions, but E-cadherin was still enriched at cytosolic regions proximal to anti-non-phosphorylated β -catenin signals. Interestingly, staining with β -catenin (indiscriminate of phosphorylation) in 48h rosettes showed enrichment at cell-cell junctions and at cytosolic regions proximal to cell-cell junctions, suggesting phosphorylated β -catenin and E-cadherin colocalize in cytoplasmic regions. Interestingly, we observed this enrichment pattern at 24h and 36h, when there is no central foci enrichment of PARD6B, which suggests cytosolic enrichment of E-cadherin occurs prior to the onset of polarization. 3D ESC cultures treated with MEK or FGFR inhibitors still demonstrated E-cadherin enrichment at cell-cell junctions and cytosolic regions (Fig. 5B), suggesting this phenotype is FGF/ERK independent.

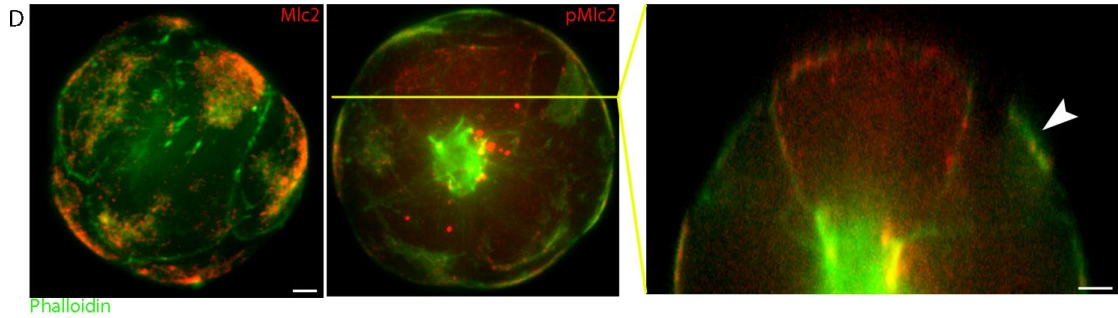
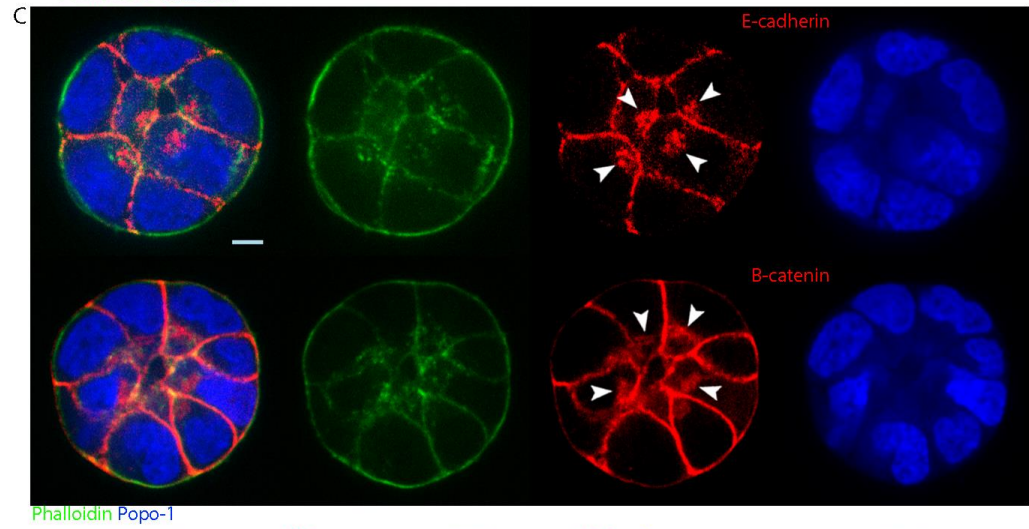
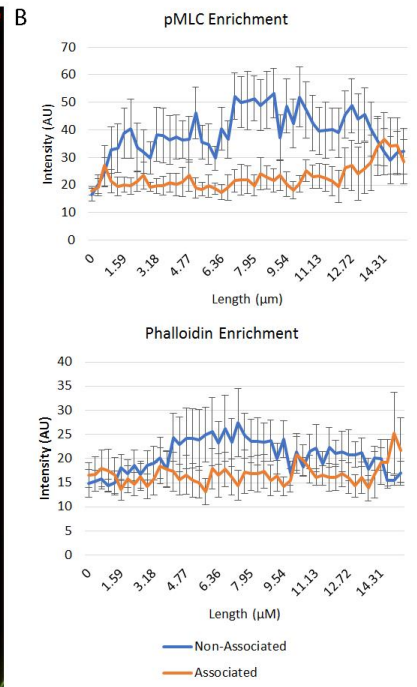
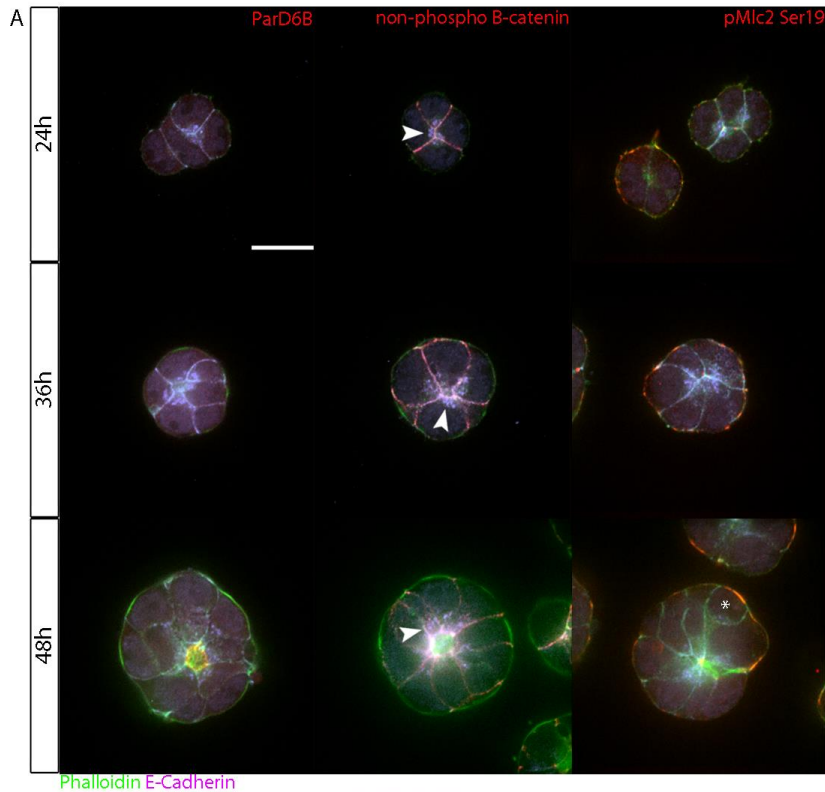


Fig. 2: 3D ESC culture progression from amorphous clusters to rosettes. Immunostaining at 24h, 36h, and 48h revealed central PARD6B membrane enrichment within clusters beginning at 48h, but not earlier (A; 20 μ m scale bar). E-cadherin staining demonstrated cell-cell junctional enrichment, but also cytoplasmic regions proximal to cell-cell junctions as early as 24h (marked with arrows). Occasional cells were observed to not be associated with the central AF in 48h clusters (*). These cells were associated with a 2.6x fold increase in cortical pMLC2 Ser19 but not phalloidin relative to their adjacent cells (B; standard error bars). 48h rosettes cell-cell junctional and cytoplasmic enrichment of E-cadherin and β -catenin (C; scale bar set at 5 μ m) 48h rosettes 3D rendered using Imaris demonstrated non-associated cells with central AF have a basal F-actin network enriched with pMLC2 Ser19 (D; indicated by arrow; 3 μ m scale bar).

At 48h, some ESC derived rosettes contain the cells that not reached at the central foci. We predicted that they must reintegrate with the central foci to maintain rosette epithelial continuity⁸⁵. To understand individual cellular dynamics and cell division patterns in the rosettes, we performed live imaging analysis on the rosettes from 48h after in the 3D condition using GPI::GFP ESCs which express the membrane tethered GFP to visualize cellular shape and movement. It was observed that mitotic cells increased cell shape roundness and migrated towards the apical domain prior to cytokinesis (Fig. 3A). To understand lateral cells movements within rosettes, GPI::GFP ESC in 3D culture were imaged at their basal domain to track basal domain movements. Indeed, tracking individual basal domains do show slight lateral migration (Fig. 3B). Interestingly, ‘new’ basal domains spontaneously appeared over time which do not appear to be from due to lateral cell movements, suggesting cells integrate from the apical-basal axis. These results suggest mitotic cells within rosettes lose their basal contact with the ECM during division and then reintegrate within the epithelium. This divisional behavior is

concatenate with mitotic epiblast cells in the post-implantation embryo, whereby mitotic epiblast cells migrate apically prior to division and reintegrate into the egg cylinder cone irrespective of their sister cell position ⁸⁶.

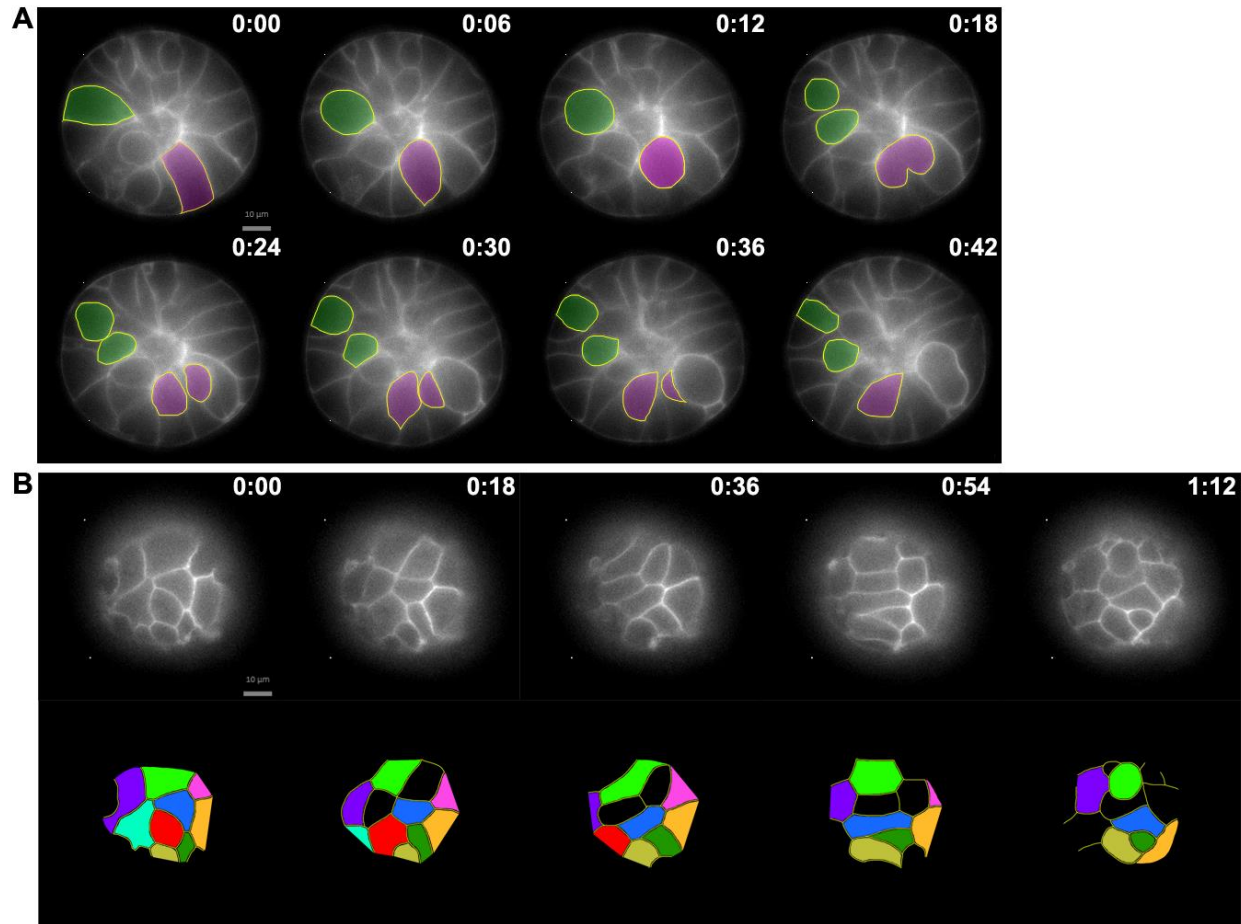


Fig. 3: GPI::GFP ESC rosette division at 48h. Center cross-section of rosette at 48h shows mitotic cells migrate towards the apical center of the rosette followed by cell division and reintegration (A). Basal cross-section of 48h rosette demonstrated basal domain migration and integration over time (B). Following individual basal domains (bottom cartoon) showed sporadic integration of new basal domains into the epithelium independent of lateral migration. Scale bar set at 10μm. Time is set to hours:mins.

Since cells within rosettes are able to reintegrate into the epithelium after mitosis, we predicted that cells within 48h rosettes which are not yet associated with the central foci will integrate into the epithelium due to actomyosin contractile forces. To answer this, rosettes were immunostained for pMlc2 pSer19 to investigate actomyosin contractility as a marker for reintegration. Indeed, comparing actin foci non-associated cells with adjacent associated cells showed a 2.6x maximal fold increase in pMlc2 pSer19 enrichment across their basal membranes ($p < 0.01$) (Fig. 2B). No statistical significant enrichment of phalloidin was observed when comparing non-associated cells with adjacent associated cells (Figure 2D). However, 3D reconstitution of 48h cysts using Imaris shows cortical phalloidin and pMLC2 enrichment in non-associated cell basal domains (Fig. 2C).

2. 3D Culture Directs ESCs into E5.5-like PEct Cells

As described above, morphology of ESCs is tightly associated with the pluripotency state, where naïve and primed pluripotent ESCs form domed and flat colonies respectively^{7,87}. Since 3D ESC cultures exhibited an epithelial morphology, we suspected 3D culturing ESC promoted naïve pluripotency exit and gain of primed-like qualities. To determine if 3D ESC cysts have exited naïve pluripotency and entered primed pluripotency, we performed qRT-PCR analyses of naïve and primed pluripotency genes over 72h in 3D culture. We used EpiSCs derived from ESCs (ESD-EpiSC), which was established from the EB differentiation protocol, as a control for primed pluripotency⁴⁶. The naïve pluripotency genes, *Rex1* and *Fgf4* showed a significant downregulation over 72h in 3D culture (0.08 ± 0.01 and 0.29 ± 0.03 fold, respectively), reaching similar expression levels to ESD-EpiSC (0.04 ± 0.01 *Rex1*; 0.27 ± 0.05 *Fgf4*) (Fig. 4A). *Nanog* is a pluripotency gene expressing in both states but higher in naïve ESCs than in primed ESCs^{88,89}. *Nanog* was also downregulated 0.26 ± 0.03 fold during 72hrs in 3D culture (Fig. 4B). On the other

hand, *Oct4*, a core pluripotency gene expressed in both naive and primed, showed relatively stable expression throughout culturing in the 3D condition. These results demonstrate that 3D culturing ESCs in the absence of 2i+Lif promotes naïve pluripotency exit.

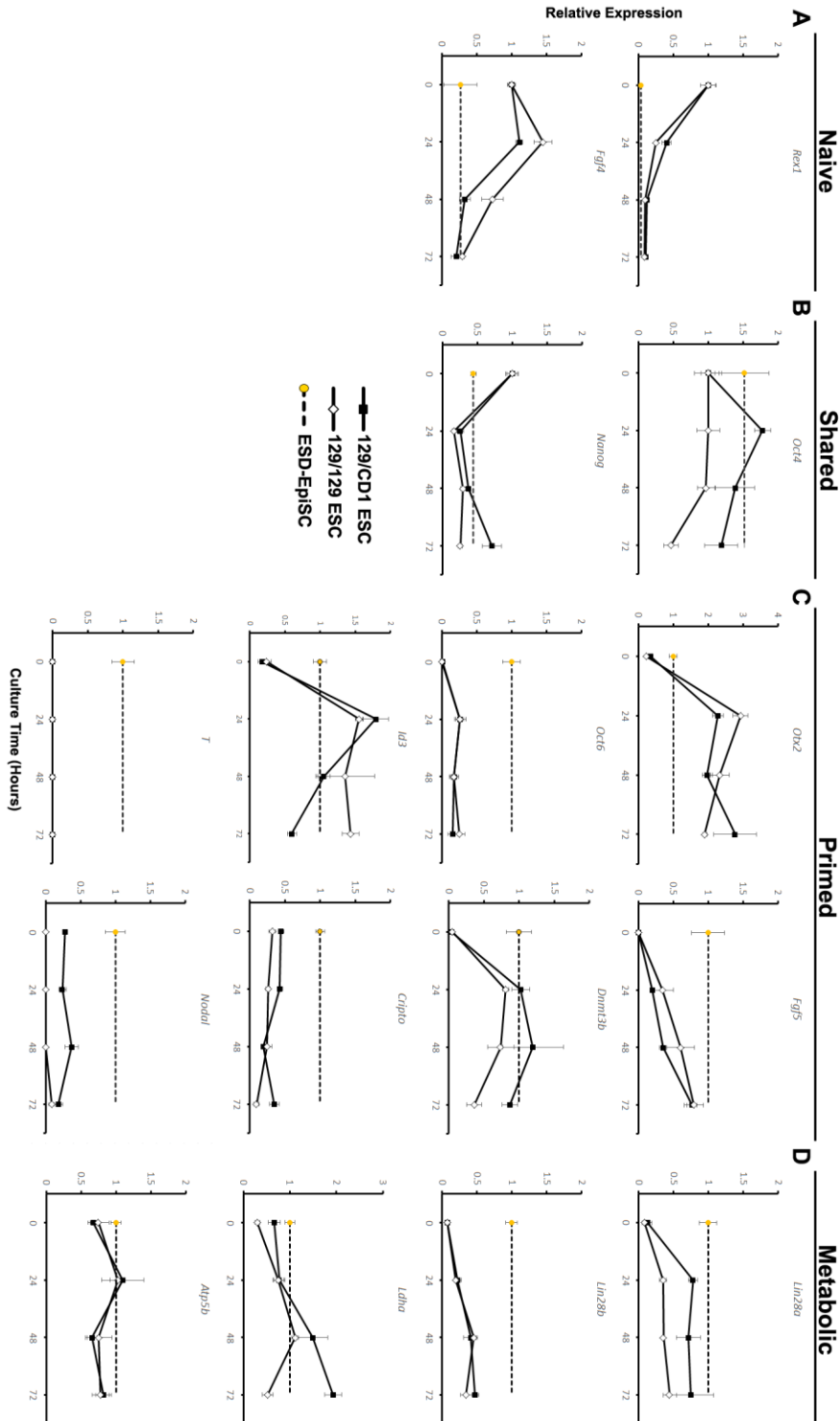


Fig. 4: qRT-PCR analysis of 3D ESC culture over 72h. 3D ESC cultures show downregulated naïve factors *Rex1* and *Fgf4* to similar levels to ESD-EpiSC (A). Shared (naïve and primed) factors *Oct4* was stably expressed, whereas *Nanog* was downregulated over 72h (B). Primed factors *Otx2*, *Fgf5*, *Dnmt3b*, and *Id3* showed significant upregulation to levels similar to ESD-EpiSC (C). Primed factor *Oct6* was weakly upregulated compared to ESD-EpiSC. TGF- β factors *Cripto* and *Nodal*, as well as Wnt/ β -catenin associated factor *T* showed no significant upregulation over 72h. Key glycolysis regulation factors *Lin28a* and *Lin28b* showed weak upregulation, but *Ldha* showed significant upregulation to levels similar to ESD-EpiSC (D). Oxidative phosphorylation associated factor *Atp5b* showed no significant change over 72h. qRT-PCR analysis was performed with 129 wt and 129/CD1 mix ESC. ESD-EpiSC are 129 wt background.

Fgf5 and *Otx2* are primed pluripotency markers, which are upregulated in E5.5 epiblast cells^{3,48,90}. *Fgf5* was upregulated over 72h in ESCs in 3D culture to the expression level comparable in ESD-EpiSCs (0.8 ± 0.1) (Fig. 4C). Interestingly, *Otx2* expression increased dramatically to 1.91 ± 0.06 fold higher than ESD-EpiSC. *Dnmt3b*, a gene encoding a *de novo* DNA methylation associated protein and primed pluripotency marker^{4,91}, was upregulated significantly from 0h to 24h, but then gradually decreased afterwards. *Oct6* is a gene encoding a TF expressed in early peri-implantation epiblast and a primed pluripotency marker^{90,92}. *Oct6* was only partial upregulated over 72h in 3D culture compared to ESD-EpiSC (0.25 ± 0.08).

Naive-to-prime pluripotency transition is tightly associated with metabolism^{7,93,94}. Naïve ESCs are bivalent and utilize both oxidative phosphorylation and glycolytic processes to meet high energy demands of rapid cell divisions and cell growth. However primed ESCs exclusively use glycolytic processes⁹⁴. We wondered if ESCs in the 3D condition adopts a primed

pluripotency and exclusively utilizes glycolysis. Metabolic regulators *Lin28a/b* have been shown to be critical for repressing oxidative phosphorylation, regulating one-carbon and nucleotide metabolism, and promoting histone methylation during EpiLC formation ⁷⁰. The levels of *Lin28a* and *Lin28b* expressions over 72h only showed modest upregulation relative to ESD-EpiSC (0.44±0.09 and 0.35±0.08 respectively) (Fig. 4D). *Ldha* (lactate dehydrogenase A), an enzyme catalyzing lactate into pyruvate and a key enzyme in aerobic glycolysis ⁹⁵, showed peak expression at 48h comparable to ESD-EpiSC. *Atp5b*, an ATP synthase associated protein and marker for oxidative phosphorylation, has been shown to be downregulated in epiblast cells from E4.5-5.5 ⁹². The expression level of *Atp5b* did not show any significant change over 72h. In summary, ESCs in 3D culture have upregulated the genes important for glycolysis compared to ESCs in 2i+Lif conditions, but still maintain the expression of the genes for oxidative phosphorylation metabolism. This suggests that 3D ESC culture directs metabolism towards glycolysis, but still retain a certain level of oxidative phosphorylation.

Nodal and Cripto are a signaling ligand and co-receptor for the Nodal signaling pathway, respectively, and are important for maintaining primed EpiSC self-renewal *in vitro* ^{7,34,96}. Brachyury (encoded in *T* gene) is a panmesodermal transcriptional factor that is regulated by Nodal and Wnt/ β -catenin signaling which is critical for PS formation ^{20,97}. To further evaluate how similar our 3D ESC derived cysts were to EpiSC we analyzed the expression of *Nodal*, *Cripto*, and *T*. Interestingly, *Nodal*, *Cripto*, and *T* showed no significant upregulation over 72h of 3D culture and were consistently very low to the expression in ESD-EpiSCs (Fig. 4C). These gene expression patterns suggest that while the ESCs in the 3D condition do exit naïve pluripotency as indicated by downregulated *Fgf4* and *Rex1*, they have not entered primed pluripotency as indicated by no significant upregulation in *Nodal*, *Cripto*, and *T* ^{7,79,98,99}. In

normal embryo development, *Otx2*, *FGF5*, *Dmmt3b*, and *Id3* are upregulated in E5.5 epiblast cells^{1,90,92}. On the other hand, *Nodal* expression is modestly increased in E4.5-5.5 epiblast cells¹. Cumulatively, these results suggest that ESCs in 3D culture most resemble PEct cells of E5.5 embryos.

3. FGF4 is required for naïve exit in 3D Culture

FGF4 is a member of the fibroblast growth factor family that activates the MAPK/ERK pathway¹⁰⁰, AKT pathway¹⁰¹, and PLC γ pathway¹⁰². *Fgf4* is essential for primitive endoderm formation in preimplantation mouse development and its expression level is a critical factor regulating the proportion of primitive endoderm and epiblast within blastocysts^{103,104}. *Fgf4* would be also necessary in peri-implantation development; *Fgf4* null embryos at E5.5 show either an undetectable, or growth restricted and highly disorganized embryo³³. Additionally, *Fgf4* is essential for differentiation of ESCs *in vitro*. The *Fgf4* null ESCs are unable to commit to multilineage differentiation which can be ameliorated with the additional of exogenous FGF4³¹.

Fibronectin-integrin signaling can also stimulate ERK2 phosphorylation via FAK-SHC-GRB2 complex^{39,41,42,44}. The ECM proteins complex with integrin heterodimers to form FAS which recruit and activates FAK via Tyr-397 autophosphorylation which is critical for Ras activation^{38,44,105}. However, FAK activation can be attenuated via synthetic RGDS peptide which directly binds with $\alpha 5\beta 1$ -integrin heterodimer to block ECM-integrin interactions^{106,107}, or by PND-1186 inhibitor which blocks Tyr-397 FAK phosphorylation⁴⁰. Since the FGF/ERK pathway has been previously shown to be critical for ESC differentiation in 2D conditions^{31,32}, we cannot rule out the possibility that 3D conditions may introduce ECM-ERK activity to promote ESC differentiation.

To determine the importance of the FGF/ERK and ECM-ERK signaling pathway in 3D ESC cyst development, we supplemented 0.02% DMSO (control), 1 μ M of PD0325981 (MEK inhibitor, MEKi), 1 μ M of PD173074 (FGFR inhibitor), 1 μ M PND-1186 (FAK inhibitor), or 10 μ M of RGDS peptide to our 3D culture media. qRT-PCR analysis over 72h revealed downregulation of both *Fgf4* and *Rex1*, for PND-1186 and RGDS treated samples to levels similar to the control (FGF4 0.21 \pm 0.08; Rex1 0.11 \pm 0.02) (Fig. 5A). However, both treatments of the MEK inhibitor (FGF4 3.76 \pm 0.78; Rex1 1.34 \pm 0.21) and the FGFR inhibitors (FGF4 1.76 \pm 0.27; Rex1 1.07 \pm 0.15) inhibited ESC showed no downregulation over 72h. Interestingly, the MEKi treated ESCs showed a 3.76 \pm 0.78 fold increase over 72h relative to ESC in the 2D 2i+Lif condition.

Imaging inhibitor treated ESC clusters at 72h revealed distinct differences in cluster morphology. Control DMSO treated ESC clusters yielded monolayer cysts with clear enrichment of PARD6B at luminal facing membrane with junctional E-cadherin (Fig. 5B). MEKi and FGFRi treated ESCs clusters developed into amorphous aggregates and showed no enrichment of PARD6B within clusters, suggesting cells are apolar. RGDS peptide treated ESC developed into a bilayered cyst with a small luminal cavity that was highly enriched for PARD6B. FAKi treated ESC clusters showed weak PARD6B enrichment on cortical surfaces within some cells. Interestingly, cytoplasmic enrichment of E-cadherin adjacent to cell-cell junctions was found in all inhibitor treated ESC clusters except FAKi, suggesting this enrichment pattern is independent of FGF/ERK signaling but dependent on FAK activity.

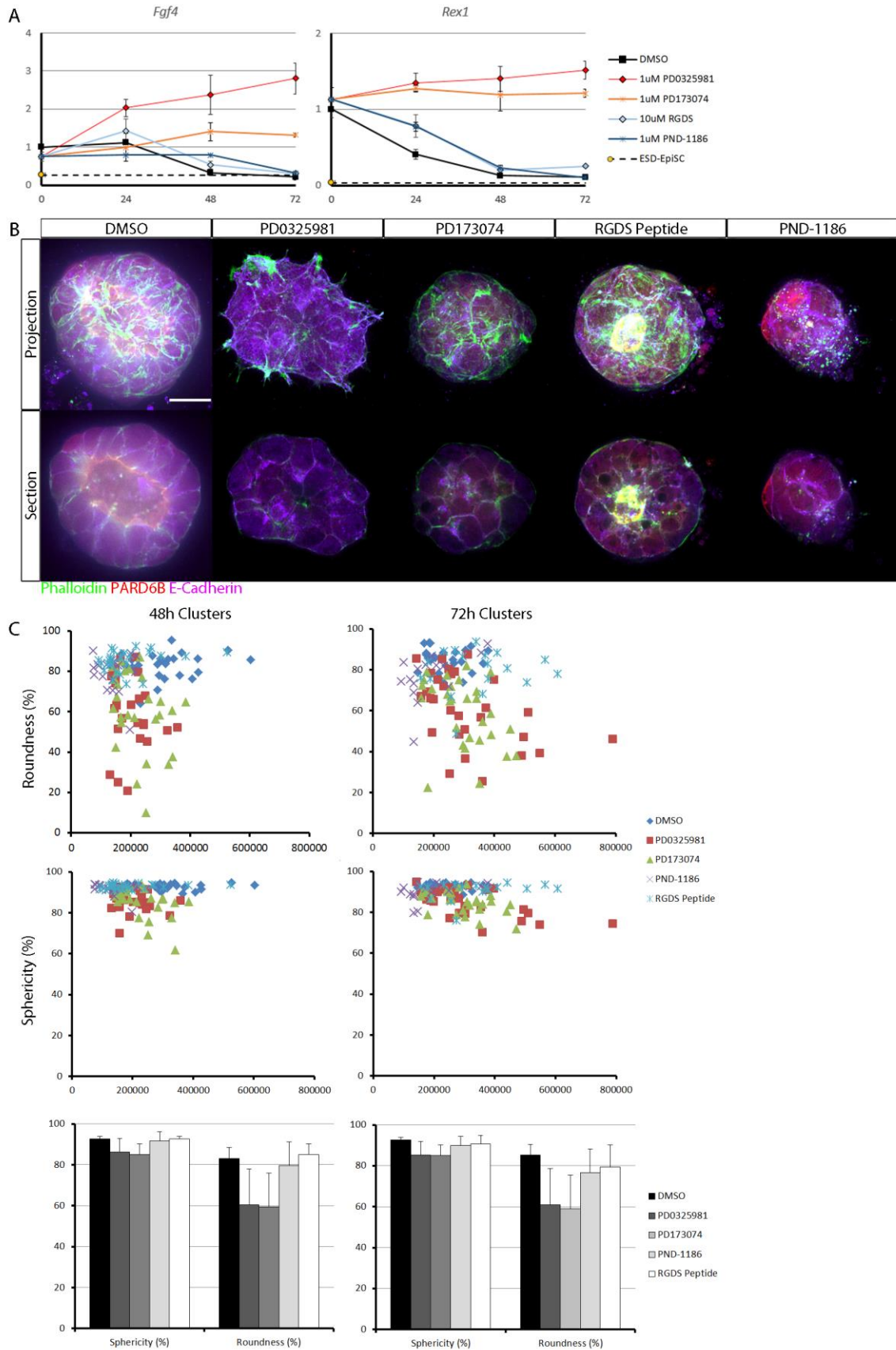


Fig. 5: Inhibitor Treatment of 3D ESC cultures show FGF/ERK but not Integrin/ERK dependence for naïve exit. 3D ESC culture was supplemented with 0.2% DMSO, 1 μ M PD0325981 (MEK inhibitor), 1 μ M PD173074 (FGFR inhibitor), 10mM RGDS peptide (Integrin inhibitor), or 1 μ M PND-1186 (FAK inhibitor). qRT-PCR analysis revealed *Fgf4* and *Rex1* was downregulated in DMSO, RGDS, and PND-1186 treated ESC but not PD0325981 or PD173074 (A). Immunostaining 72h 3D ESC cultures showed DMSO treated samples formed monolayer cysts with PARD6B enriched luminal membranes, and E-cadherin enriched cell-cell junctions (B). PD0325981 and PD173074 treated ESC formed amorphous clusters with no PARD6B membrane staining. RGDS peptide treated ESC formed bilayer cysts with small lumens enriched for PARD6B staining. PND-1186 treated ESC formed clusters with cortical PARD6B membrane staining in some cells. All clusters were enriched for E-cadherin at cell-cell junctions; all clusters were enriched for E-cadherin at cytoplasmic regions proximal to cell-cell junctions except PND-1186 treated ESC clusters. Quantifying cluster roundness and sphericity using Icy showed DMSO, RGDS, peptide, and PND-1186 treated ESC formed highly round and spherical clusters at 48h and 72h timepoints (C). PD0325981 and PD173074 treated ESC formed clusters with relatively lower roundness and sphericity at both timepoints.

The control cysts were typically found with highly spherical and round contour morphology. Yet, MEKi and FGFRi treated clusters showed amorphous organization and irregular cortical roundness suggesting FGF/ERK signaling promotes high cortical roundness. Quantification of cyst morphology at 48h and 72h (Fig. 5C) revealed MEKi and FGFRi treated clusters had lower sphericity and roundness (72h Mek inhibited $61\pm 17\%$ $p < 0.0001$; Fgfr inhibited $59\pm 17\%$ $p < 0.0001$) compared to control (72h Roundness = $85\pm 5\%$). FAKi and RGDS treated clusters showed no significant difference compared to the control at 48h or 72h.

Endogenous *Fgf4* is necessary for ESC differentiation in 2D culture³¹. To determine if auto- and paracrine FGF4 is necessary for 3D ESC naïve exit and monolayer cysts formation, we established *Fgf4*^{wt/wt}, *Fgf4*^{wt/del}, and *Fgf4*^{del/del} B6 ESCs to address this question. In 2i+Lif 2D conditions, *Fgf4*^{wt/wt} and *Fgf4*^{wt/del} ESCs grew in domed colonies, however *Fgf4*^{del/del} ESCs cultured as flat monolayer. This was not ameliorated with low (20ng/mL) or high (100ng/mL) exogenous FGF2/4 and Hep (1ug/mL) after 48h (Fig. 6A). qRT-PCR analysis these lines in 2i+Lif with or without supplemented FGF2/4+Hep showed four times lower *Rex1* expression compared to 129 wt and 129/CD1 ESC (Fig. 6B). Yet similar expression levels of *Oct4* and *Nanog* was observed in all conditions and lines, suggesting strain differences in gene expression between B6 and 129 ESC lines. Interestingly, three passages of *Fgf4*^{del/del} ESCs in 2i+Lif with supplemented 50ng/mL FGF4 and 1µg/mL Hep could restore domed colony morphology, suggesting an unidentified role of *Fgf4* in naïve pluripotency (Fig. 6C).

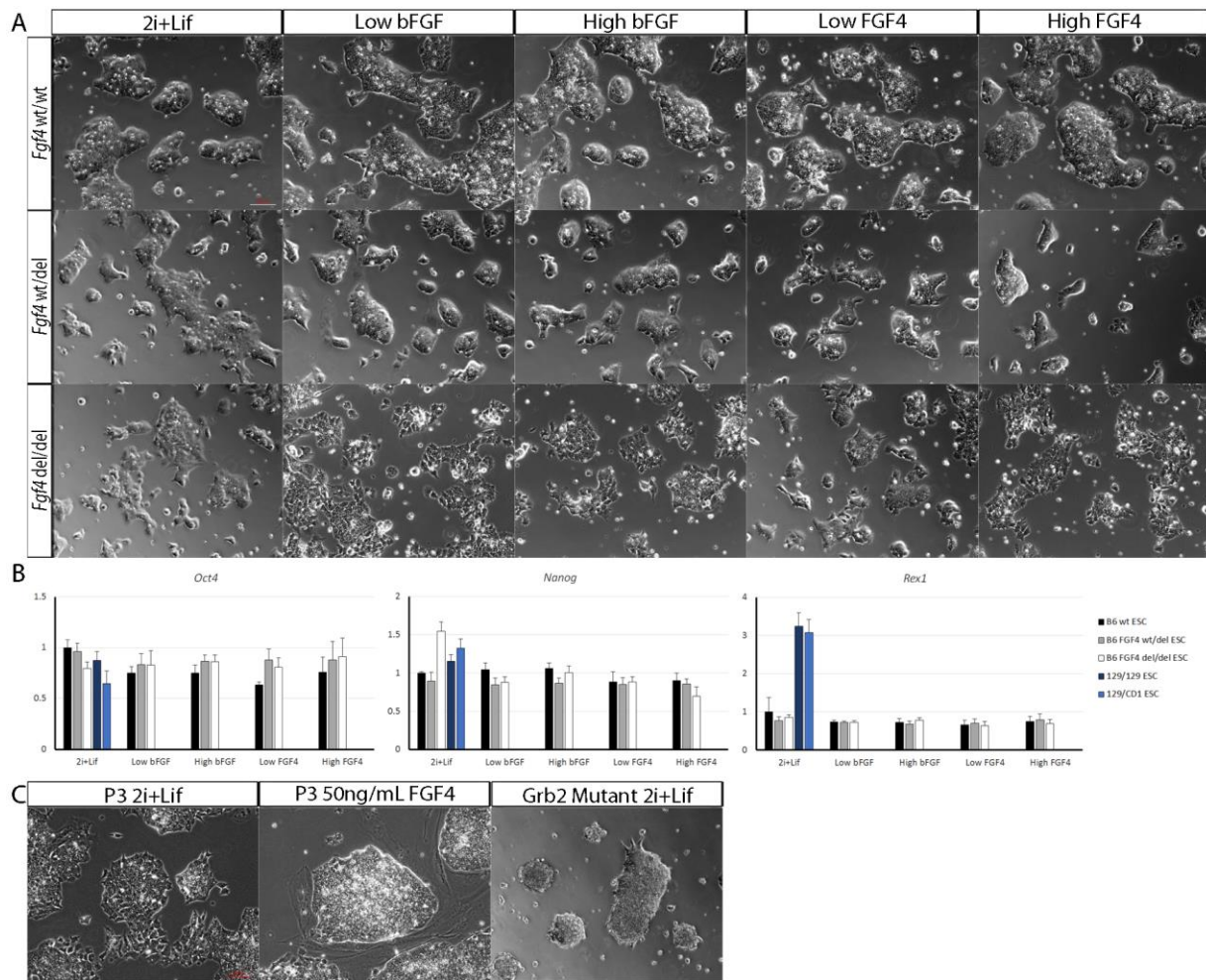


Fig. 6: B6 *Fgf4*^{del/del} ESC exhibit flat morphology in 2i+Lif conditions. Culturing B6 *Fgf4*^{wt/wt}, *Fgf4*^{wt/del}, *Fgf4*^{del/del} ESC on gelatin coated dishes in 2i+Lif showed domed colony morphology in *Fgf4*^{wt/wt} and *Fgf4*^{wt/del} ESC, however *Fgf4*^{del/del} demonstrated flat colony formation (A). Culturing in the presence of 2i+Lif with supplemented Heparin (1μg/mL) and either bFGF or FGF4 in low (20ng/mL) or high (100ng/mL) conditions for 48h did not rescue domed shaped morphology in *Fgf4*^{del/del} ESC. qRT-PCR analysis of B6 lines in all conditions showed similar levels of *Oct4* and *Nanog* across all conditions compared to 129 wt and 129/CD1 ESC, however *Rex1* expression was significantly lower in B6 lines regardless of FGF2/4+Heparin supplementation (B). Culturing *Fgf4*^{del/del} ESC in 2i+Lif with supplemented

FGF4+Heparin (50ng/mL; 1µg/mL respectively) over three passages rescued domed shaped morphology compared to just 2i+Lif conditions (C). *Grb2* mutant ESC in 2i+Lif conditions demonstrated domed colony formation. Scale bars set at 100µm.

Culturing *Fgf4*^{wt/wt} ESC in 3D culture for 72h yielded monolayer cysts identical to 129 wt ESC (Fig. 7A), with antibody staining for PARD6B and Laminin enriched at luminal and cortical membranes respectively. Supplementation of Fgf4+Hep yielded identical cyst clusters and staining patterns. Contrastingly, 3D *Fgf4*^{del/del} ESC cultures formed amorphous colonies with either ‘salt and pepper’ cytosolic ParD6B enrichment, or central foci enrichment. No *Fgf4*^{del/del} cluster was observed to have a central lumen, suggesting endogenous Fgf4 is required for lumen formation, but dispensable for ParD6B expression in 3D culture. However, *Fgf4*^{del/del} colonies were enriched with cortical laminin, suggesting FGF4/ERK activity is independent of basal membrane formation. Upon Fgf4+Hep supplementation, *Fgf4*^{del/del} ESCs developed into cysts similar to *Fgf4*^{wt/wt} ESCs. Interestingly, 3D *Fgf4*^{wt/del} ESC cultures developed into small monolayer cysts with cortical PARD6B staining, exclusive of laminin signal. Clusters were also observed to have an invaginated cup-like morphology with a cavity open to the ECM from the central lumen. This morphology was rescued upon FGF4+Hep supplementation, suggesting monolayer cyst formation is FGF4/ERK gradient dependent. qRT-PCR analysis revealed 72h 3D *Fgf4*^{wt/wt} and *Fgf4*^{wt/del} ESC cultures downregulated *Nr0b1*—a naïve pluripotency marker—compared to 2i+Lif conditions, but *Fgf4*^{del/del} did not suggesting 3D *Fgf4*^{del/del} ESC culture doesn’t promote naïve pluripotency exit (Fig. 7B). Analysis of *Nr0b1* was selected as an indicator of naïve pluripotency exit since *Rex1* expression is not significantly downregulated in 3D B6 *Fgf4*^{wt/wt} ESC culture over 72h (0.56±0.7 fold decrease) compared to 129wt ESC (0.08±0.01 fold decrease) (Fig. 7C). This difference is likely due to strain differences since

Nr0b1 was downregulated in B6 *Fgf4*^{wt/wt} over 72h (0.009±0.004 fold decrease) (Fig. 7C). Supplemented FGF4+Hep rescued *Nr0b1* downregulation in 3D *Fgf4*^{del/del} ESC culture. *Nanog* was similarly rescued and downregulated to levels similar to FGF4^{wt/wt} (serum 1.4±0.2 fold decrease; Fgf4+Hep 3.8±0.4 fold decrease).

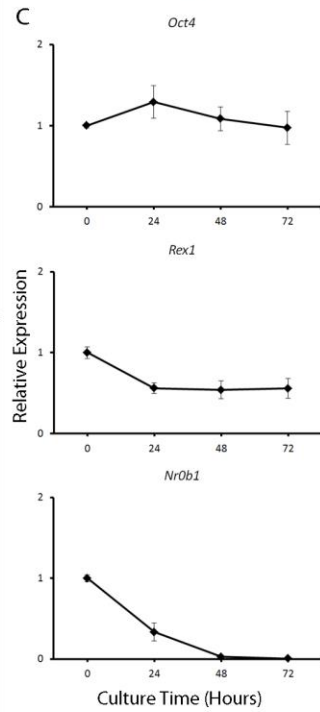
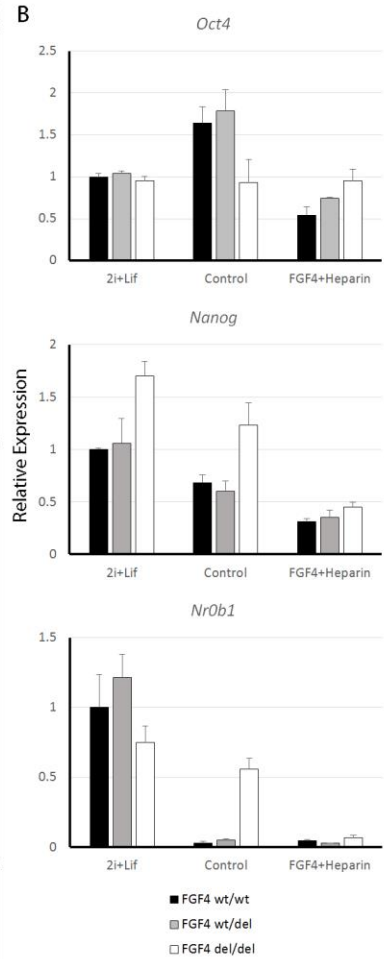
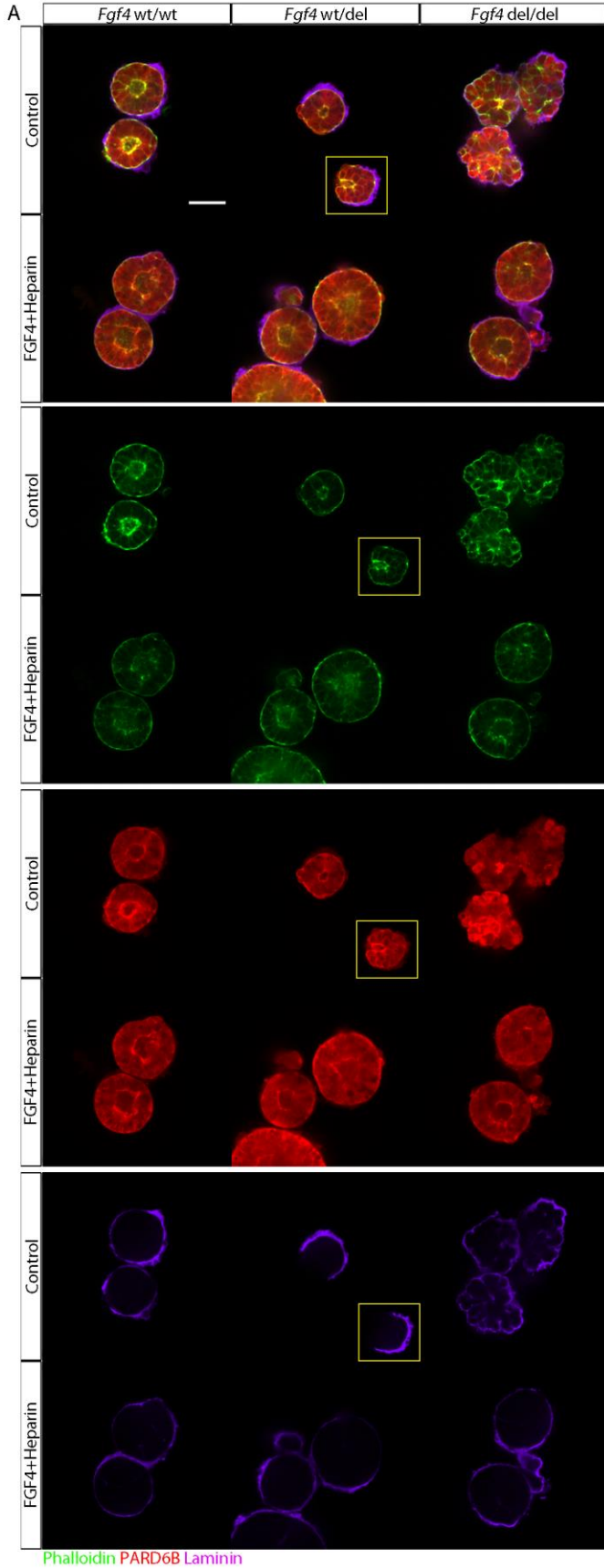


Fig. 7: Endogenous *Fgf4* Expression is critical for naïve exit and cyst formation. 3D *Fgf4*^{wt/wt}, *Fgf4*^{wt/del}, *Fgf4*^{del/del} ESC culture with or without supplemented FGF4+Hep (50ng/mL; 1μg/mL respectively) for 72h. *Fgf4*^{wt/wt} ESC formed monolayer cysts with luminal membrane enrichment of PARD6B and basal membrane enrichment of laminin (A). No significant difference was observed with supplemented FGF4+Hep. *Fgf4*^{wt/del} formed small monolayer cysts with cortical enrichment of PARD6B which was mutually exclusive with Laminin staining. Cysts were also observed to have a cup-like morphology with its internal lumen exposed to the outer ECM. FGF4+Hep supplementation rescued this morphology to *Fgf4*^{wt/wt}. *Fgf4*^{del/del} ESC formed amorphous aggregates with weak cytosolic PARD6B enrichment and Laminin enriched cortical staining; some clusters were found to have internal PARD6B enriched membranes. FGF4+Hep supplementation rescued monolayer cyst morphology. qRT-PCR analysis of 72h 3D ESC culture and 2D ESC culture in 2i+Lif on gelatin for *Oct4*, *Nanog*, and *Nr0b1* showed relatively stable expression of *Oct4* throughout all conditions (B). *Nanog* was significantly downregulated in 3D *Fgf4*^{wt/wt} and *Fgf4*^{wt/del} ESC culture but not *Fgf4*^{del/del}. However, this was rescued with exogenous FGF4+Hep supplementation. Similarly, *Nr0b1* expression was downregulated in *Fgf4*^{wt/wt} and *Fgf4*^{wt/del} ESCs in 3D culture but not *Fgf4*^{del/del} ESC, which was rescued when supplemented with FGF4+Hep. qRT-PCR analysis of *Fgf4*^{wt/wt} over 72h hours shows stable expression of *Oct4*, downregulated *Nr0b1*, but weakly downregulated *Rex1* (C). Scale bars set at 50μm.

To further demonstrate that FGF/ERK signaling is required for naïve-exit in 3D culture, we established a 129/CD1 *Grb2* mutant ESCs using CRISPR-Cas9 technology. Sequencing revealed a 234bp insertion allele within the third exon of the first protein coding region in one allele and a 3pb deletion corresponding to Leu25 deletion in the other. nBLAST analysis yielded

no high homology results for the insertion. Leu25 has been previously annotated as a “major contributors to the variable size of the core of SH3 domain”, and has been shown to H-bond with Ala23, Asp23, and Val27¹⁰⁸. N-SH3 has been shown to be the major binding domain of GRB2 towards SOS, as P49L point mutation in N-SH3 of GRB2 has been shown to have significantly lower binding with SOS¹⁰⁹. Contrary to *Fgf4*^{del/del} in 2i+Lif, *Grb2* mutant ESC formed domed colonies further suggesting a link between Fgf4 and naïve pluripotency morphology independent of FGF/ERK signaling (Fig. 6C). However, 3D *Grb2* mutant ESC cultures developed amorphous aggregates compared to wt ESC at 72h (Fig. 8A). Most aggregate showed weak cytosolic enrichment of PARD6B, but occasional cyst-like clusters were present with highly enriched PARD6B luminal staining. This is likely due to the single copy GRB2 Leu deletion allele still retaining some GRB2-SOS binding activity, since similar structural impairments (eg. P49L GRB2) still retained low level GRB2-SOS complexing¹⁰⁹. All *Grb2* mutant clusters demonstrated cortical laminin staining, suggesting basal membrane formation is independent of GRB2/ERK signaling, concatenate with our FGF4^{del/del} ESC results. qRT-PCR quantification of 3D *Grb2* mutant ESC culture over 72h revealed maintained *Oct4* expression, modestly downregulated *Fgf4* and *Rex1* (0.53±0.05 and 0.67±0.13 respectively), and minimally upregulated *Fgf5* (18±4 fold increase) compared to 129 wt ESC (248±66 fold increase) (Fig. 8B). These results indicate our *Grb2* mutant was overall not able to exit naïve in 3D culture similar to FGFR inhibition, MEK inhibition, and *Fgf4*^{del/del} ESC, suggesting GRB2/ERK signaling is critical for naïve exit in 3D culture.

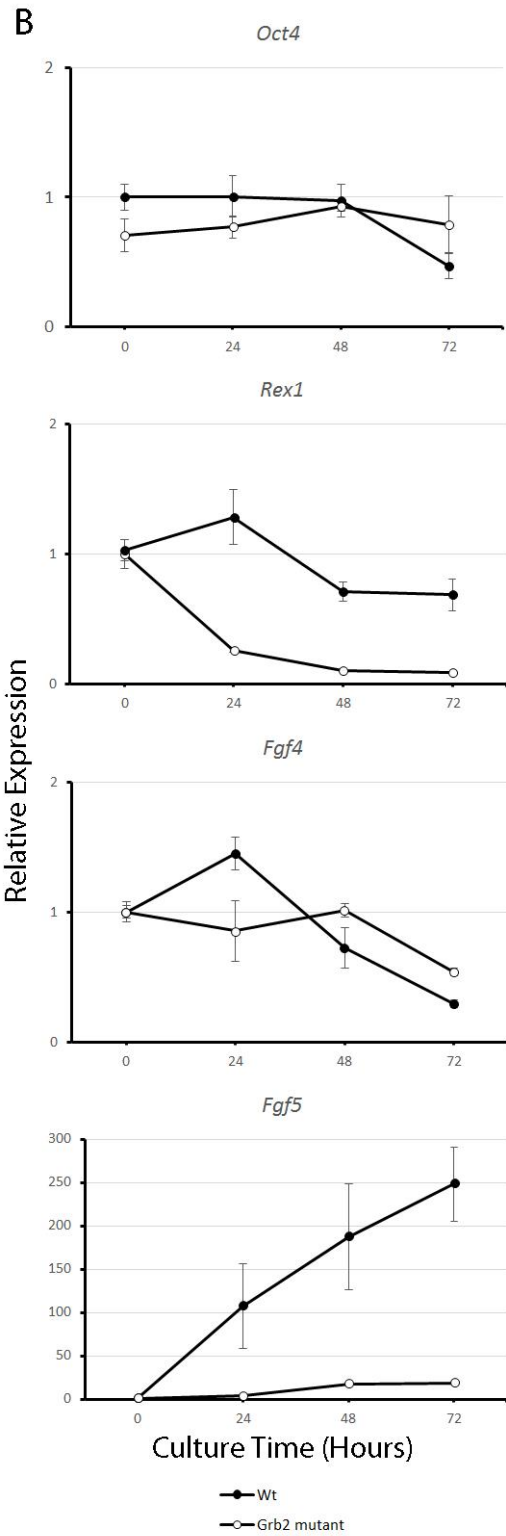
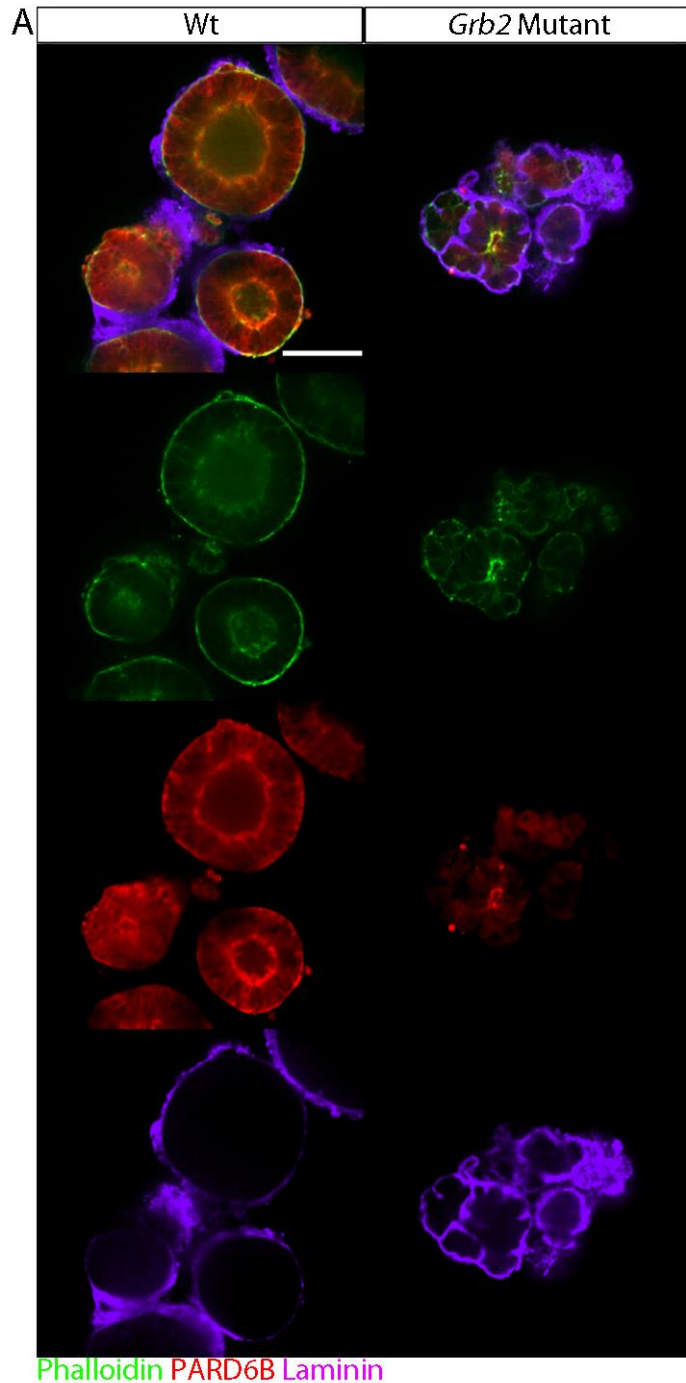


Fig. 8: Grb2 is critical for 3D ESC culture naïve exit and cyst formation. 3D Wt and *Grb2* mutant ESC culture for 72h. Wt ESC formed monolayer cysts with luminal membrane enriched PARD6B and basal membrane enriched Laminin (A). *Grb2* mutant ESC formed amorphous aggregates weak cytosolic or strong luminal enriched PARD6B; clusters also demonstrated basal membrane enriched Laminin. qRT-PCR analysis of wt and *Grb2* mutant ESC over 72h showed relatively stable expression of *Oct4* (B). Wt exhibited significantly downregulated for *Rex1* and *Fgf4*, while *Grb2* mutant ESC was weakly downregulated for both. Wt showed significant upregulated *Fgf5*, but *Grb2* mutant ESC was only weakly upregulated. Scale bar set at 20 μ m.

4. ECM Promotes ESC Polarization in 2D Culture without Lif+2i

Integrin-ECM interactions are critical for peri-implantation inner cell mass development and EB formation⁵⁰⁻⁵². ECMs have been described in two modalities: ECM stiffness, and ECM composition. ECM stiffness has been shown to modulate hESC differentiation into mesodermal lineages via Wnt pathway signaling and may play a key role in naïve pluripotency exit¹¹⁰. ECM composition provided by specific α and β integrin subunit complexing with a specific ECM molecule also plays a role in ESC differentiation (ie. ECM molecular cues promote cell polarization). Embryos lacking β 1-integrin were embryonic lethal during implantation, suggesting ECM molecular cues are critical for embryonic development⁵¹. Additionally, β 1-integrin null ESC in matrigel 3D culture has been shown to ablate monolayer cyst development and yielded amorphous clusters with cortical PARD6B enrichment, similar to wt 3D ESC cultures in agarose¹². Indeed, differentiation of ESCs in 2D culture has been shown to highly depend on the types of ECM coated on a plastic plate, demonstrating ECM-integrin interactions have a critical role in ESC differentiation^{36,111}. To elucidate the role of ECM molecular cues on PEct-like cell morphology and polarization, FGF4^{wt/wt}, FGF4^{wt/del}, FGF4^{del/del} B6 ESCs were

plated on gelatin, collagen, laminin fragment, fibronectin, or Matrigel coated glass-bottom plates. 2D culture was employed to control for variable stiffness which is difficult to control in 3D culture.

WT *Fgf4*^{wt/wt} B6ESCs in 2D cultures at 72h in the absence of 2i+Lif showed ECM substrate dependent morphologies. The ESCs cultured on gelatin and collagen coated plates yielded similar monolayer colonies with weak apical PARD6B and aPKC enrichment (Fig. 9A). They showed columnar-like epithelial colonies with elongated columnar-like cells localized in the center and relatively shorter columnar-like cells in the periphery. Contrastingly, the ESCs cultured on fibronectin formed uniform squamous-like monolayer colonies with strong PARD6B and aPKC apical enrichment. Similar to gelatin and collagen coated conditions, the ESCs cultured on a laminin coated plate yielded columnar-like monolayer colonies with weak PARD6B and aPKC enrichment. Interestingly, ESC cultured on Matrigel formed cup-like colonies with central concavities highly enriched for PARD6B and aPKC. Peripheral cells not associated with the central concavities showed no apical PARD6B or aPKC enrichment. *Fgf4*^{wt/del} B6ESCs yielded similar morphologies to *Fgf4*^{wt/wt} across all ECM conditions, except with relatively lower enrichment of PARD6B and aPKC in all conditions. As expected, *Fgf4*^{del/del} showed no significant PARD6B or aPKC apical enrichment for all conditions we examined. Additionally, *Fgf4*^{del/del} B6ESCs throughout all conditions showed relatively low cell-cell contact, with frequent spaces within colonies between cells. Colonies were also observed appear as a ‘bumpy’ monolayer, where individual cells exhibited lower height to the ECM at their cell-cell junctions compared to their centers. Interestingly, *Fgf4*^{del/del} ESCs plated on laminin occasionally formed domed aggregate colonies. Cells embedded within these aggregate colonies (ie. Cells with cell-cell and/or cell-ECM junctions throughout their entire cell membrane) were observed with high

cytosolic or membrane enriched PARD6B and aPKC. However, surface cells on these aggregates (ie. Cells exposed to the surrounding media) were however not enriched for PARD6B or aPKC.

Supplementation of FGF4+Hep demonstrated interesting changes in $Fgf4^{wt/wt}$ 2D culture. $Fgf4^{wt/wt}$ on gelatin and collagen formed domed colonies, instead of monolayer epithelium, with cortical PARD6B and aPKC enrichment (Fig. 9B). When plated on laminin, $Fgf4^{wt/wt}$ ESC formed squamous-like monolayer, similar to fibronectin in the absence of exogenous FGF4+Hep, and showed relatively strong apical enrichment of F-actin but unchanged levels of PARD6B and aPKC enrichment. $Fgf4$ +Hep supplementation showed no significant effect on $Fgf4^{wt/wt}$ in fibronectin or Matrigel 2D conditions. These effects were similarly seen for $Fgf4^{wt/del}$ with supplemented $Fgf4$ +Hep, except for colonies in the laminin coated plates forming columnar-like epithelium instead of squamous-like. Interestingly, FGF4+Hep supplementation did not rescue $Fgf4^{del/del}$ morphology or polarization relative to $Fgf4^{wt/wt}$ in the majority of ECM conditions assayed. $Fgf4^{del/del}$ ESC with exogenous FGF4+Hep in gelatin, collagen, fibronectin, and laminin exhibited similar colony morphology compared to serum only conditions. PARD6B and aPKC immunostaining showed no significant enrichment at apical membranes, but sporadic cytosolic enrichment was observed in some cells within colonies. However, $Fgf4^{del/del}$ ESCs cultured on a Matrigel coated plates with $Fgf4$ +Hep supplementation formed domed colonies with a small enclosed central lumen strongly enriched for PARD6B and aPKC, contrasting the cup-like colonies in $Fgf4^{wt/wt}$.

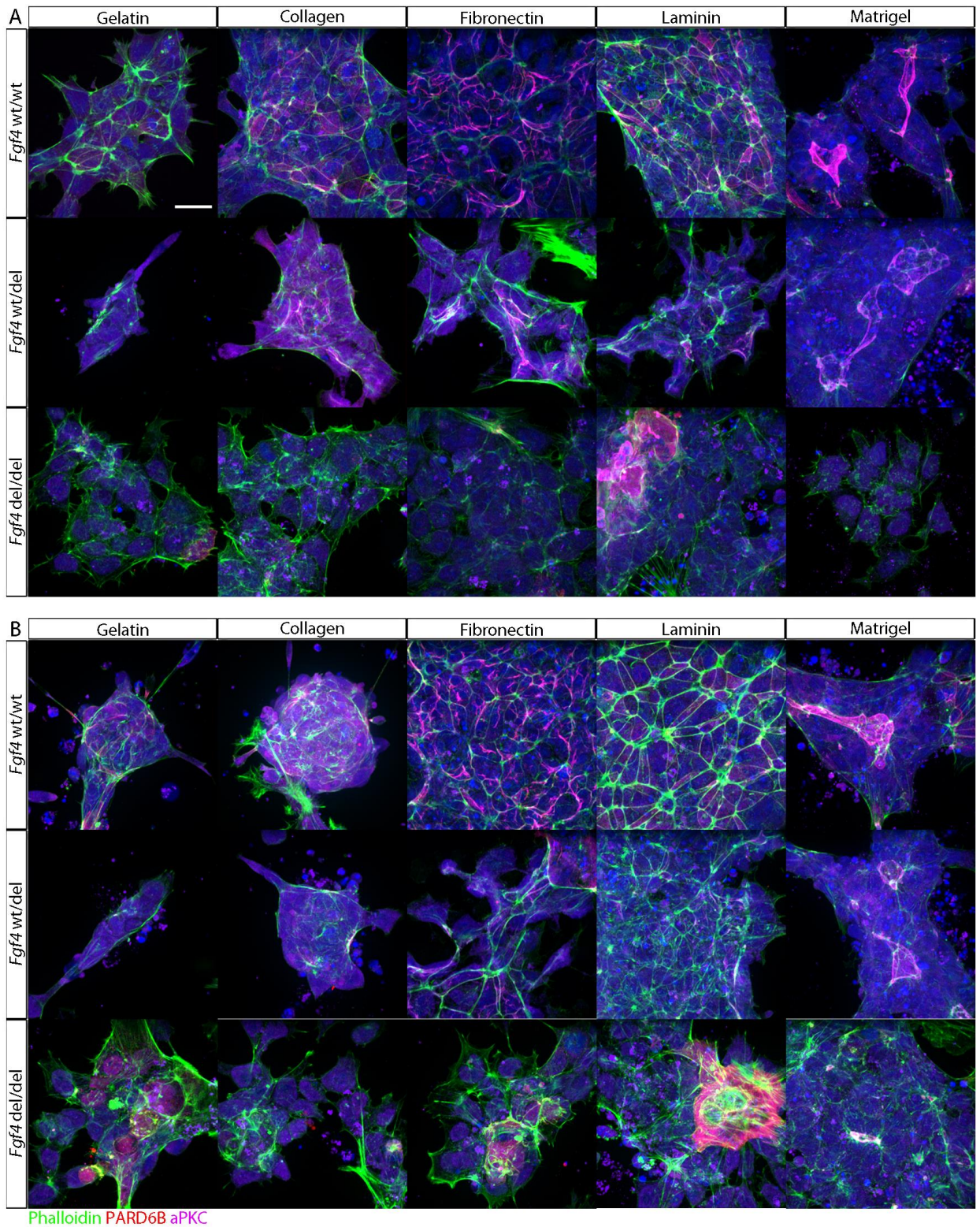


Fig. 9: ECM and endogenous *Fgf4* expression regulates morphology and polarization in 2D ESC culture. 2D *Fgf4*^{wt/wt}, *Fgf4*^{wt/del}, and *Fgf4*^{del/del} ESC plated on either gelatin, collagen,

fibronectin, laminin, or Matrigel for 72h in 2i+Lif free conditions (A). FGF4+Hep (50ng/mL and 1µg/mL respectively) was supplemented (B). Scale bar set at 50µm.

Discussion

ESCs are recognized for their potential in regenerative medicine because of their pluripotency to differentiate into all cell types within the adult body. For the first 20 years after the discovery of ESCs, the most challenging issue was maintaining their pluripotent state *in vitro*. However, identification of several factors including Lif^{112,113}, BMP4¹¹⁴, and 2i¹¹⁵ conditions allowed for reliable derivation and maintenance of ground state ESCs *in vitro*. However, the largest barrier limiting medical application of ESCs is their difficulty in differentiating into clinically viable cells in high numbers. This limitation is in part due to the reliance on EB formation for initial differentiation of ESCs, which is difficult to control due to their complex cell-cell interactions in EBs causing unregulated differentiation into all three germ layers which lowers ESC differentiation into specific cell types^{21,23}. 2D ESC differentiation protocols have been explored to ameliorate this with varying success. 2D ESC culture with supplemented bFGF have been shown to be a reliable protocol for neurectoderm differentiation⁷¹. However, this is suggested to be the ‘default’ pathway for ESC differentiation in the absence of other factors. 2D hematopoietic differentiation may be achieved by plating ESC on a stromal layer^{69,70}. However hematopoietic differentiation efficiency is <1%, and is dependent on the stromal cell line and passage number of ESCs. A more competent, reliable, and efficient ESC differentiation strategy is necessary to fully utilize ESC in clinical work.

Here we show 3D culturing of ESCs from the naive state produces PEct-like cells with similar morphology. ESCs cultured in the 3D culture condition self-organize into a rosette through establishing cell polarity within 48h. The rosettes cavitated to form a monolayer cyst

by 72h concatenate with PEct formation *in vivo*. Downregulation of naïve pluripotency markers, including *Rex1*, *FGF4*, *Nr0b1*, and *Nanog* indicating an exit of pluripotency by 72hr. The cysts show an upregulation of PEct markers such as *Fgf5*, *Id3*, *Otx2*, and *Dmnt3b*. They also showed a weak upregulation of *Lin28a/b* compared to ESD-EpiSC indicating an exit from bivalent metabolism (ie. Equal oxidative phosphorylation and glycolysis for energy demands) and upregulation of glycolysis. However, ESCs in 3D culture show no significant upregulation of *T*, *Nodal*, or *Cripto* which are key markers of primed pluripotency. These gene expression trends suggest 3D ESC cultures have exited naïve pluripotency but have not entered primed pluripotency.

It was observed that E-cadherin and β -catenin was localized at cell-cell junctions and at cytosolic regions proximal to cell-cell junctions as indicated by counter staining with anti-non-phosphorylated β -catenin. This cytosolic enrichment pattern was observed even in 3D ESC cultures that were MEK and FGFR inhibited, suggesting cytosolic E-cadherin enrichment was independent of FGF/ERK activity and naïve exit. It is interesting to speculate that cytosolic E-cadherin and β -catenin plays a role in rosette formation. It was observed that mitotic cells round-up, migrate to the apical surface, divide, and reintegrate into the epithelium. Occasionally, cells within 48h rosettes were observed to not be associated with the central foci and had enriched pMLC2 Ser19 at their basal domains suggesting contractility. We speculate that post-mitotic cells that are actively integrating into the rosette and associate with the inner foci, utilize two mechanisms of reintegration: basal actomyosin contractility, and apical E-cadherin adhesion. Basal contractility within non-foci associated cells increases cell internal pressure, which applies omnidirectional force to surrounding cell-cell junctions. Since surrounding lateral cells apply an equal but opposite force to counteract this force, and the basal contractility is maintaining the

interal pressure, lateral movement and cell extrusion from the rosette is limited. However, longitudinal movement towards the central foci is likely less inhibited from neighboring cell-cell junctions and thus the force generated from basal contractility promotes cellular extension towards the central foci. It may be that E-cadherin and β -catenin cytosolic enrichment facilitates rapid cytoskeletal turnover along the elongated axis to promote cell extension. However, the persistence E-cadherin at cytosolic regions prior to polarization, as marked by PARD6B staining, suggests that E-cadherin cytosolic localization proximal to cell-cell junctions may facilitate PAR protein localization for correct polarization axis initiation.

Surprisingly, *Fgf4^{del/del}* ESC formed flat monolayer colonies in 2i+Lif whereas *Fgf4^{wt/wt}* and *Fgf4^{wt/del}* formed domed colonies, typical of naïve pluripotency. This could not be rescued upon FGF4+Hep supplementation after 48h, but was after three passages. However, Grb2 mutant ESC demonstrated typical domed colonies in 2i+Lif conditions, suggesting FGF4/ERK pathway is not responsible for this morphology. FGF4 stimulation may also activate Jak/Stat, PLC γ , and PI3K/Akt pathways. We predict that Akt activation through FGF4 is responsible for domed morphology in naïve cells, and ablation of FGF4 will result in a monolayer morphology. Akt3 has been described as an essential regulator of cell survival and proliferation in ESC ¹¹⁶. Blocking Akt activity via chemical inhibitors or shRNA has been shown to increase cell apoptosis. Although we did not observe any difference in cell apoptosis in *Fgf4^{del/del}* compared to *Fgf4^{wt/wt}*, Akt activation is multifaceted and may be compensated by non-growth factor stimulants (e.g. ECM-integrin signaling) ^{105,117}. Indeed, Akt inactivation has been shown to induce morphological changes in other cell types, such as promoting elongation in vascular endothelial cells ^{118,119}.

Endogenous FGF4/ERK activity has been reported to be critical for ESC differentiation into neural cells³¹. Assaying if auto- and paracrine FGF4 is required for ESC differentiation in cyst formation in 3D culture, *Fgf4*^{del/del} formed amorphous clusters after 72h and were still enriched for *Nr0b1*, suggesting they did not exit naïve pluripotency. *Fgf4*^{wt/del} formed monolayer cysts with cortical PARD6B enrichment that were mutually exclusive with Laminin staining; cup-like clusters were also observed, whereby the lumen of these cysts was exposed to the surrounding ECM. These suggest that strong endogenous FGF4 activity is required for proper cyst formation. It is interesting to speculate if FGF4 not only promotes ESC naïve exit, but also promotes actin polymerization which is necessary for cyst formation in 3D culture. This was suggested in 2D *Fgf4*^{wt/wt} ESC culture with supplemented FGF4+Hep showed increased apical F-actin enrichment when plated Laminin and Fibronectin compared to just serum. Additionally, FGF4^{wt/wt} colonies plated on gelatin and collagen formed domed colonies with supplemented FGF4+Hep compared to monolayer colonies in just serum, suggesting over stimulation of FGF4 regulates colony morphology. Perhaps FGF4 promotes Rac-dependent actin polymerization in 3D culture to promote cyst formation. Weak FGF4 stimulation results in weak F-actin polymerization thus hindering cell reintegration after division. This would lead to poor maintenance of epithelial continuity and thus promote morphological cluster abnormalities such as cup-like clusters. It is unknown how cortical apical domain formation, as indicated by cortical enrichment of PARD6B, plays a role in this hypothesis and whether it is a precursor to cup-like clusters or a separate morphological outcome because of low FGF4 stimulation.

ECM-integrin interactions have been demonstrated to promote Erk2 phosphorylation via FAK/c-SRC/SHC2/GRB2 complex to promote SOS-dependent Ras activation^{39,42,44}. However, when we assayed if ECM/Erk2 activation plays a role ESC differentiation in 3D culture by

inhibiting integrin and FAK with RGDS peptide and PND-1186 inhibitor respectively, ESCs were still able to downregulate naïve factors *Rex1* and *Fgf4* suggesting naïve exit. However, PND-1186 treated ESC in 3D culture did prevent cyst formation and yielded colonies with cortical PARD6B enriched membranes. It seems that ECM-integrin interactions don't promote naïve exit in 3D ESC culture with 2i+Lif removal, but does regulate cluster morphology. This is clearly exemplified when 2D *Fgf4*^{wt/wt} ESC culture without 2i+Lif in a variety of different ECM coated glass-bottom plates resulting in different morphologies. Since ECM-integrin interactions have been shown to play a significant role in directing ECM differentiation ³⁶, the different morphologies observed in 2D ESC cultures are likely unique cell types being differentiated. However, this raises the question of what ECM-integrin interaction is critical for PEct-like cell differentiation? Previous reports have shown β_1 -integrin as being critical for proper cyst formation in 3D ESC culture ¹³. Additionally, ESC differentiated in suspension with Fibronectin have shown to generate EpiLC that are functionally competent to form PGCLC, suggesting fibronectin- $\alpha_5\beta_1$ integrin interactions is important for EpiLC formation. Developmentally, laminin chains α_1 , β_1 , γ_1 , nidogen-1/2, α_1 collagen IV, and perlecan have been identified as part of the E7.0 ectodermal basement membrane. *Lama1*^{-/-} embryos were shown to maintain egg-cylinder cone morphology at E6.5 but quickly degenerate at E7.5 ¹²⁰. Since ablation of LAMA1 was not restricted to just the ectodermal basement membrane, it is unclear if laminin is necessary for PEct maintenance or whole embryo survival.

Conclusion & Future Directions

In this study, we have demonstrated that ESC in 3D culture develop into monolayer cysts by 72h with luminal apical domain orientation. qRT-PCR analysis of cysts demonstrated naïve exit over 72h as observed with downregulated *Rex1* and *Fgf4*. PEct associated factors including

Otx2, *Fgf5*, *Oct6*, *Dnmt3b*, and *Id3* were upregulated, but TGF- β associated *Nodal* and *Cripto* were not upregulated suggesting cysts have not entered primed pluripotency. Inhibition of FGF/ERK pathway but not Integrin/FAK blocked naïve exit, suggesting naïve exit in 3D culture is dependent FGF/ERK pathway. Morphological analysis of FGF/ERK inhibited ESC in 3D culture show blockage of polarization and cyst formation, as well as disruption of colony sphericity and roundness, suggesting a link between naïve exit and cyst formation. *Fgf4*^{del/del} ESC in 3D culture similarly were not able to exit naïve pluripotency as observed with retained *Nr0b1* expression, suggesting autocrine/paracrine FGF4 is critical for naïve exit in 3D culture and cyst formation. Additionally, Grb2 mutant ESC 3D culture were not able to exit naïve pluripotency and formed amorphous aggregates, suggesting the FGF4/ERK pathway is required for cyst formation. Plating *Fgf4*^{wt/wt}, *Fgf4*^{wt/del}, and *Fgf4*^{del/del} onto gelatin, collagen, fibronectin, laminin, and Matrigel coated dishes without 2i+Lif demonstrated ECM-dependent polarization morphology, with the strongest ParD6B and aPKC staining from fibronectin coated dishes. *Fgf4*^{del/del} were not able to polarize when plated on any of the assayed ECM conditions even when supplemented with FGF4+Heparin, suggesting an underlying requirement of FGF4 stimulation during naïve pluripotency for polarization upon 2i+Lif removal.

Although qRT-PCR analysis of ESC in 3D culture show gene expression highly similar to PEct cells *in vivo*, a functional assay is required to demonstrate their potency for EpiSC formation. This can be accomplished by 3D culturing ESC with or without additional activin A, then replating onto 2D conditions in CDM media to isolate EpiSC colonies, and comparing to traditional ESC-derived EpiSC techniques and 2i+Lif conditions. It was interesting to observe that *Fgf4*^{del/del} ESC in 2i+Lif form flat colonies compared to domed wt ESC colonies. This may be linked with the observed lack of polarization of *Fgf4*^{del/del} ESC when supplemented with

FGF4+Hep on various ECM coated dishes. We hypothesize FGF4 stimulation is important for activated Akt in priming naïve ESC for polarization upon 2i+Lif removal. This can be explored further by analyzing Akt phosphorylation in *Fgf4*^{del/del} ESC with and without supplemented FGF4+Heparin in 2i+Lif conditions and assaying their potential for polarization when 2D cultured on various ECM coated dishes without 2i+Lif. Additionally, it is recommended to observe how FGF4+Heparin regulates cytoskeletal reorganization in *Fgf4*^{del/del} ESC within 2i+Lif conditions as observed by the rescue of domed morphology over successive passaging. It is interesting to speculate that FGF4 may increase cortical contractility in ESC colonies to promote domed morphology, whereas lack of FGF4 downregulates cytoskeletal contractility and subsequently promotes flat ESC morphology. Overall, we recommend pursuing the morphological changes caused by FGF4 within naïve ESC and 3D ESC cultures.

Appendix

Mouse Training Theory Certificate



University Animal Care Committee
Office of the Vice-principal
(Research and international relations)
Animal Compliance Office
McGill University
James Administration Building, Room 429
845 Sherbrooke St. West
Montreal (Quebec), Canada H3A 2T5

Comité universitaire de protection des animaux
Bureau du Vice-principal
(Recherche et relations internationales)
Bureau de déontologie animale
Université McGill
Pavillon James de l'administration, bureau 429
845, rue Sherbrooke Ouest
Montréal, Québec, Canada H3A 2T5

 (514) 398-2639
 (514) 398-4644
 animalcare@mcgill.ca

July 27, 2017

The McGill University Animal Care Committee certifies that

Kwong, Aaron

has successfully completed a

Theory Course

Comprising

Advanced Theory Course

Completed on

September 3, 2014

This certificate is issued on behalf of the University Animal Care Committee using the secure Animal Care Program database. Please contact the Animal Care Training Administrator at (514) 398-2639 or animalcare@mcgill.ca if there is a need to authenticate this document.

Animal Compliance Office

Mouse Workshop Certificate



University Animal Care Committee
Office of the Vice-principal
(Research and international relations)
Animal Compliance Office
McGill University
James Administration Building, Room 429
845 Sherbrooke St. West
Montreal (Quebec), Canada H3A 2T5

Comité universitaire de protection des animaux
Bureau du Vice-principal
(Recherche et relations internationales)
Bureau de déontologie animale
Université McGill
Pavillon James de l'administration, bureau 429
845, rue Sherbrooke Ouest
Montréal, Québec, Canada H3A 2T5

 (514) 398-2639
 (514) 398-4644
 animalcare@mcgill.ca

July 27, 2017

The McGill University Animal Care Committee certifies that

Kwong, Aaron

has successfully completed a

Mouse Workshop

Comprising

Mouse Cardiac Puncture
Mouse Cervical Dislocation Euthanasia with Anesthesia
Mouse Cervical Dislocation Euthanasia without Anesthesia
Mouse Handling and Restraint

Completed on

September 18, 2014
September 18, 2014
January 9, 2015
September 18, 2014

This certificate is issued on behalf of the University Animal Care Committee using the secure Animal Care Program database. Please contact the Animal Care Training Administrator at (514) 398-2639 or animalcare@mcgill.ca if there is a need to authenticate this document.

Animal Compliance Office

Bibliography

1. Boroviak, T., Loos, R., Bertone, P., Smith, A. & Nichols, J. The ability of inner-cell-mass cells to self-renew as embryonic stem cells is acquired following epiblast specification. *Nat. Cell Biol.* **16**, 516–28 (2014).
2. Kojima, Y. *et al.* The transcriptional and functional properties of mouse epiblast stem cells resemble the anterior primitive streak. *Cell Stem Cell* **14**, 107–120 (2014).
3. Buecker, C. *et al.* Reorganization of enhancer patterns in transition from naive to primed pluripotency. *Cell Stem Cell* **14**, 838–53 (2014).
4. Leitch, H. G. *et al.* Naive pluripotency is associated with global DNA hypomethylation. *Nat. Struct. Mol. Biol.* **20**, 311–6 (2013).
5. Smith, Z. D. *et al.* A unique regulatory phase of DNA methylation in the early mammalian embryo. *Nature* **484**, 339–344 (2012).
6. Schulz, E. G. *et al.* The Two Active X Chromosomes in Female ESCs Block Exit from the Pluripotent State by Modulating the ESC Signaling Network (Supplementary). **14**,
7. Fiorenzano, A. *et al.* Cripto is essential to capture mouse epiblast stem cell and human embryonic stem cell pluripotency. *Nat. Commun.* **7**, 12589 (2016).
8. Huang, Y., Osorno, R., Tsakiridis, A. & Wilson, V. In Vivo Differentiation Potential of Epiblast Stem Cells Revealed by Chimeric Embryo Formation. *Cell Rep.* **2**, 1571–1578 (2012).
9. Wu, J. *et al.* Stem cells and interspecies chimaeras. *Nature* **540**, 51–59 (2016).
10. Smith, A. Formative pluripotency: the executive phase in a developmental continuum. *Development* **144**, 365–373 (2017).
11. Morgani, S., Nichols, J. & Hadjantonakis, A.-K. The many faces of Pluripotency: in vitro adaptations of a continuum of in vivo states. *BMC Dev. Biol.* **17**, 7 (2017).
12. Bedzhov, I. & Zernicka-Goetz, M. Self-organizing properties of mouse pluripotent cells initiate morphogenesis upon implantation. *Cell* **156**, 1032–44 (2014).
13. Bedzhov, I. & Zernicka-Goetz, M. Self-organizing properties of mouse pluripotent cells initiate morphogenesis upon implantation. *Cell* **156**, 1032–1044 (2014).
14. Bryant, D. M. *et al.* A Molecular Switch for the Orientation of Epithelial Cell Polarization. *Dev. Cell* 1–17 (2014). doi:10.1016/j.devcel.2014.08.027
15. Meder, D., Shevchenko, A., Simons, K. & Füllekrug, J. Gp135/podocalyxin and NHERF-2 participate in the formation of a preapical domain during polarization of MDCK cells. *J. Cell Biol.* **168**, 303–313 (2005).
16. Funayama, N. S. *et al.* β -Catenin Regulates Primitive Streak Induction through Collaborative Interactions with SMAD2/SMAD3 and OCT4. *Cell Stem Cell* **16**, 639–652 (2015).
17. Vincent, S. D., Dunn, N. R., Hayashi, S., Norris, D. P. & Robertson, E. J. Cell fate decisions within the mouse organizer are governed by graded Nodal signals. *Genes Dev.*

- 17**, 1646–1662 (2003).
18. Arnold, S. J. & Robertson, E. J. Making a commitment: cell lineage allocation and axis patterning in the early mouse embryo. *Nat. Rev. Mol. Cell Biol.* **10**, 91–103 (2009).
 19. Hospital, G., Street, T., Gard, T., Hoge, E. A. & Kerr, C. Extra-embryonic Wnt3 regulates the establishment of the primitive streak in mice. **6**, 356–372 (2015).
 20. Turner, D. a, Rué, P., Mackenzie, J. P., Davies, E. & Martinez Arias, A. Brachyury cooperates with Wnt/ β -catenin signalling to elicit primitive-streak-like behaviour in differentiating mouse embryonic stem cells. *BMC Biol.* **12**, 63 (2014).
 21. Hong, S. H., Werbowetski-Ogilvie, T., Ramos-Mejia, V., Lee, J. B. & Bhatia, M. Multiparameter comparisons of embryoid body differentiation toward human stem cell applications. *Stem Cell Res.* **5**, 120–130 (2010).
 22. Kurosawa, H. Methods for inducing embryoid body formation: in vitro differentiation system of embryonic stem cells. *J. Biosci. Bioeng.* **103**, 389–398 (2007).
 23. Moon, S. H. *et al.* Optimizing human embryonic stem cells differentiation efficiency by screening size-tunable homogenous embryoid bodies. *Biomaterials* **35**, 5987–5997 (2014).
 24. Keller, G. M. In vitro differentiation of embryonic stem cells. *Curr. Opin. Cell Biol.* **7**, 862–869 (1995).
 25. Chen, Y., Li, X., Eswarakumar, V. P., Seger, R. & Lonai, P. Fibroblast growth factor (FGF) signaling through PI 3-kinase and Akt/PKB is required for embryoid body differentiation. *Oncogene* **19**, 3750–3756 (2000).
 26. Lanner, F. *et al.* Heparan sulfation-dependent fibroblast growth factor signaling maintains embryonic stem cells primed for differentiation in a heterogeneous state. *Stem Cells* **28**, 191–200 (2010).
 27. Doughton, G., Wei, J., Tapon, N., Welham, M. J. & Chalmers, A. D. Formation of a polarised primitive endoderm layer in embryoid bodies requires Fgfr/Erk signalling. *PLoS One* **9**, (2014).
 28. Hamazaki, T., Kehoe, S. M., Nakano, T. & Terada, N. The Grb2/Mek pathway represses Nanog in murine embryonic stem cells. *Mol. Cell. Biol.* **26**, 7539–49 (2006).
 29. Cheng, A. M. *et al.* Mammalian Grb2 regulates multiple steps in embryonic development and malignant transformation. *Cell* **95**, 793–803 (1998).
 30. Kraushaar, D. C., Yamaguchi, Y. & Wang, L. Heparan sulfate is required for embryonic stem cells to exit from self-renewal. *J. Biol. Chem.* **285**, 5907–5916 (2010).
 31. Kunath, T. *et al.* FGF stimulation of the Erk1/2 signalling cascade triggers transition of pluripotent embryonic stem cells from self-renewal to lineage commitment. *Development* **134**, 2895–902 (2007).
 32. Molotkov, A., Mazot, P., Brewer, J. R., Cinalli, R. M. & Soriano, P. Distinct Requirements for Fgfr1 and Fgfr2 in Primitive Endoderm Development and Exit from Pluripotency. *Dev. Cell* **41**, 511–526.e4 (2017).

33. Feldman, B., Poueymirou, W., Papaioannou, V. E., DeChiara, T. M. & Goldfarb, M. Requirement of FGF-4 for postimplantation mouse development. *Science* (80-.). **267**, 246–9 (1995).
34. Vallier, L., Alexander, M. & Pedersen, R. a. Activin/Nodal and FGF pathways cooperate to maintain pluripotency of human embryonic stem cells. *J. Cell Sci.* **118**, 4495–4509 (2005).
35. Greber, B. *et al.* FGF signalling inhibits neural induction in human embryonic stem cells. *EMBO J.* **30**, 4874–4884 (2011).
36. Wang, H., Luo, X. & Leighton, J. Extracellular Matrix and Integrins in Embryonic Stem Cell Differentiation. **8**, 15–21 (2015).
37. Kinbara, K., Goldfinger, L. E., Hansen, M., Chou, F.-L. & Ginsberg, M. H. Ras GTPases: integrins' friends or foes? *Nat. Rev. Mol. Cell Biol.* **4**, 767–778 (2003).
38. Toutant, M. *et al.* Alternative Splicing Controls the Mechanisms of FAK Autophosphorylation. *Mol. Cell. Biol.* **22**, 7731–7743 (2002).
39. Schlaepfer, D. D., Jones, K. C. & Hunter, T. Multiple Grb2-mediated integrin-stimulated signaling pathways to ERK2/mitogen-activated protein kinase: summation of both c-Src- and focal adhesion kinase-initiated tyrosine phosphorylation events. *Mol. Cell. Biol.* **18**, 2571–85 (1998).
40. Tanjoni, I. *et al.* PND-1186 FAK inhibitor selectively promotes tumor cell apoptosis in three-dimensional environments. *Cancer Biol. Ther.* **9**, 764–777 (2010).
41. Mitra, S. K., Hanson, D. A. & Schlaepfer, D. D. Focal adhesion kinase: in command and control of cell motility. *Nat. Rev. Mol. Cell Biol.* **6**, 56–68 (2005).
42. Schlaepfer, D. D., Hanks, S. K., Hunter, T. & van der Geer, P. Integrin-mediated signal transduction linked to Ras pathway by GRB2 binding to focal adhesion kinase. *Nature* **372**, 786–791 (1994).
43. Meakin, S. O., MacDonald, J. I. S., Gryz, E. A., Kubu, C. J. & Verdi, J. M. The signaling adapter FRS-2 competes with Shc for binding to the nerve growth factor receptor TrkA: A model for discriminating proliferation and differentiation. *J. Biol. Chem.* **274**, 9861–9870 (1999).
44. Schlaepfer, D. D. & Hunter, T. Focal adhesion kinase overexpression enhances Ras-dependent integrin signaling to ERK2/mitogen-activated protein kinase through interactions with and activation of c-Src. *J. Biol. Chem.* **272**, 13189–13195 (1997).
45. Gamba, G. *et al.* G Protein-coupled Receptors Mediate Two Functionally Distinct Pathways of Tyrosine Phosphorylation in Rat 1a Fibroblasts. **272**, 31648–31656 (1997).
46. Zhang, K. *et al.* Distinct functions of BMP4 during different stages of mouse ES cell neural commitment. *Development* **137**, 2095–105 (2010).
47. Pelton, T. A., Sharma, S., Schulz, T. C., Rathjen, J. & Rathjen, P. D. Transient pluripotent cell populations during primitive ectoderm formation: correlation of in vivo and in vitro

- pluripotent cell development. *J. Cell Sci.* **115**, 329–339 (2002).
48. Khoa, L. T. P. *et al.* Visualization of the epiblast and visceral endodermal cells using Fgf5-P2A-venus BAC transgenic mice and epiblast stem cells. *PLoS One* **11**, 1–15 (2016).
 49. Abe, K. *et al.* Endoderm-Specific Gene Expression in Embryonic Stem Cells Differentiated to Embryoid Bodies. *Exp. Cell Res.* **229**, 27–34 (1996).
 50. Liu, J. *et al.* Integrins are required for the differentiation of visceral endoderm. *J. Cell Sci.* **122**, 233–242 (2009).
 51. Stephens, L., Sutherland, A. & Klimanskaya, I. Deletion of beta 1 integrins in mice results in inner cell mass failure and peri-implantation lethality. *Genes Dev.* 1883–1895 (1995). doi:10.1101/gad.9.15.1883
 52. Moore, R., Tao, W., Smith, E. R. & Xu, X.-X. The primitive endoderm segregates from the epiblast in $\beta 1$ integrin-deficient early mouse embryos. *Mol. Cell. Biol.* **34**, 560–72 (2014).
 53. Rathjen, J. *et al.* Formation of a primitive ectoderm like cell population, EPL cells, from ES cells in response to biologically derived factors. *J. Cell Sci.* **112** (Pt 5, 601–12 (1999).
 54. Rathjen, J. Identification of a Biological Activity That Supports Maintenance and Proliferation of Pluripotent Cells from the Primitive Ectoderm of the Mouse. *Biol. Reprod.* **69**, 1863–1871 (2003).
 55. Brons, I. G. M. *et al.* Derivation of pluripotent epiblast stem cells from mammalian embryos. *Nature* **448**, 191–5 (2007).
 56. Bai, J., Ching, C. B., Chowbay, B. & Chen, W. N. Secreted protein profile from HepG2 cells incubated by S(-) and R(+) enantiomers of chiral drug warfarin - An analysis in cell-based system and clinical samples. *Proteomics - Clin. Appl.* **4**, 808–815 (2010).
 57. Lewis, J. A., Dennis, W. E., Hadix, J. & Jackson, D. A. Analysis of secreted proteins as an in vitro model for discovery of liver toxicity markers. *J. Proteome Res.* **9**, 5794–5802 (2010).
 58. Choi, S. *et al.* Proteomic analysis of proteins secreted by HepG2 cells treated with butyl benzyl phthalate. *J. Toxicol. Environ. Health. A* **73**, 1570–85 (2010).
 59. Yamashita, R. *et al.* Extracellular proteome of human hepatoma cell, HepG2 analyzed using two-dimensional liquid chromatography coupled with tandem mass spectrometry. *Mol. Cell. Biochem.* **298**, 83–92 (2007).
 60. Gardner, R. L., Lyon, M. F., Evans, E. P. & Burtenshaw, M. D. Clonal analysis of X-chromosome inactivation and the origin of the germ line in the mouse embryo. *J. Embryol. Exp. Morphol.* **88**, 349–63 (1985).
 61. Hayashi, K., Ohta, H., Kurimoto, K., Aramaki, S. & Saitou, M. Reconstitution of the mouse germ cell specification pathway in culture by pluripotent stem cells. *Cell* **146**, 519–532 (2011).
 62. Schulz, E. G. *et al.* The two active X chromosomes in female ESCs block exit from the

- pluripotent state by modulating the ESC signaling network. *Cell Stem Cell* **14**, 203–16 (2014).
63. Nakaki, F. *et al.* Induction of mouse germ-cell fate by transcription factors in vitro. *Nature* **501**, 222–6 (2013).
 64. Lawson, K. A. *et al.* Bmp4 is required for the generation of primordial germ cells in the mouse embryo. *Genes Dev.* **13**, 424–436 (1999).
 65. Hayashi, K. & Surani, M. A. Self-renewing epiblast stem cells exhibit continual delineation of germ cells with epigenetic reprogramming in vitro. *Development* **136**, 3549–3556 (2009).
 66. Van Winkle, A. P., Gates, I. D. & Kallos, M. S. Mass transfer limitations in embryoid bodies during human embryonic stem cell differentiation. *Cells Tissues Organs* **196**, 34–47 (2012).
 67. Choi, Y. Y. *et al.* Controlled-size embryoid body formation in concave microwell arrays. *Biomaterials* **31**, 4296–4303 (2010).
 68. Nostro, M. C., Cheng, X., Keller, G. M. & Gadue, P. Wnt, Activin, and BMP Signaling Regulate Distinct Stages in the Developmental Pathway from Embryonic Stem Cells to Blood. *Cell Stem Cell* **2**, 60–71 (2008).
 69. Lim, W. F., Inoue-Yokoo, T., Tan, K. S., Lai, M. & Sugiyama, D. Hematopoietic cell differentiation from embryonic and induced pluripotent stem cells. *Stem Cell Res. Ther.* **4**, 71 (2013).
 70. Weisel, K. C., Gao, Y., Shieh, J. H. & Moore, M. A. S. Stromal cell lines from the aorta-gonado-mesonephros region are potent supporters of murine and human hematopoiesis. *Exp. Hematol.* **34**, 1505–1516 (2006).
 71. Ying, Q.-L., Stavridis, M., Griffiths, D., Li, M. & Smith, A. Conversion of embryonic stem cells into neuroectodermal precursors in adherent monoculture. *Nat. Biotechnol.* **21**, 183–186 (2003).
 72. Abranches, E. *et al.* Neural differentiation of embryonic stem cells in vitro: A road map to neurogenesis in the embryo. *PLoS One* **4**, (2009).
 73. Murry, C. E. & Keller, G. Differentiation of Embryonic Stem Cells to Clinically Relevant Populations: Lessons from Embryonic Development. *Cell* **132**, 661–680 (2008).
 74. Yeh, J. J. *et al.* Culturing Three Dimensional MDCK cells for Analyzing Intracellular Dynamics. **8**, 834–843 (2010).
 75. Veazey, K. J. & Golding, M. C. Selection of stable reference genes for quantitative RT-PCR comparisons of mouse embryonic and Extra-Embryonic stem cells. *PLoS One* **6**, (2011).
 76. Trott, J. & Arias, A. M. Single cell lineage analysis of mouse embryonic stem cells at the exit from pluripotency. (2013). doi:10.1242/bio.20135934
 77. Tabuse, Y. *et al.* Atypical protein kinase C cooperates with PAR-3 to establish embryonic

- polarity in *Caenorhabditis elegans*. *Development* **125**, 3607–3614 (1998).
78. Joberty, G., Petersen, C., Gao, L. & Macara, I. G. The cell-polarity protein Par6 links Par3 and atypical protein kinase C to Cdc42. *Nat. Cell Biol.* **2**, 531–9 (2000).
 79. Nichols, J. & Smith, A. Naive and primed pluripotent states. *Cell Stem Cell* **4**, 487–92 (2009).
 80. Wray, J., Kalkan, T. & Smith, A. G. The ground state of pluripotency. *Biochem. Soc. Trans.* **38**, 1027–32 (2010).
 81. Furuse, M., Fujita, K., Hiragi, T., Fujimoto, K. & Tsukita, S. Claudin-1 and -2: novel integral membrane proteins localizing at tight junctions with no sequence homology to occludin. *J. Cell Biol.* **141**, 1539–1550 (1998).
 82. Stevenson, B. R., Siliciano, J. D., Mooseker, M. S. & Goodenough, D. A. Identification of ZO-1: a high molecular weight polypeptide associated with tight junction (zonula occludens) in a. *J. Cell Biol* **103**, 755–766 (1986).
 83. Riethmacher, D., Brinkmann, V. & Birchmeier, C. A targeted mutation in the mouse E-cadherin gene results in defective preimplantation development. *Proc. Natl. Acad. Sci. U. S. A.* **92**, 855–9 (1995).
 84. Nelson, W. J. Regulation of cell-cell adhesion by the cadherin-catenin complex. *Biochem. Soc. Trans.* **36**, 149–55 (2008).
 85. Bergstrahl, D. T., Lovegrove, H. E. & St Johnston, D. Lateral adhesion drives reintegration of misplaced cells into epithelial monolayers. *Nat. Cell Biol.* **17**, 1497–1503 (2015).
 86. Gardner, R. L. & Cockroft, D. L. Complete dissipation of coherent clonal growth occurs before gastrulation in mouse epiblast. *Development* **125**, 2397–2402 (1998).
 87. Collier, A. J. *et al.* Comprehensive Cell Surface Protein Profiling Identifies Specific Markers of Human Naive and Primed Pluripotent States. *Cell Stem Cell* 1–17 (2017). doi:10.1016/j.stem.2017.02.014
 88. Murayama, H. *et al.* Successful Reprogramming of Epiblast Stem Cells by Blocking Nuclear Localization of β -Catenin. *Stem Cell Reports* **4**, 1–11 (2014).
 89. Zhang, H. MLL1 Inhibition Reprograms Epiblast Stem Cells to Naive Pluripotency. *Stem Cell* **18**, 481–494 (2016).
 90. Acampora, D. *et al.* Loss of the Otx2-Binding Site in the Nanog Promoter Affects the Integrity of Embryonic Stem Cell Subtypes and Specification of Inner Cell Mass-Derived Epiblast. *Cell Rep.* **15**, 2651–2664 (2016).
 91. Ficiz, G. *et al.* FGF signaling inhibition in ESCs drives rapid genome-wide demethylation to the epigenetic ground state of pluripotency. *Cell Stem Cell* **13**, 351–9 (2013).
 92. Boroviak, T. *et al.* Lineage-Specific Profiling Delineates the Emergence and Progression of Naive Pluripotency in Mammalian Embryogenesis. *Dev. Cell* **35**, 366–382 (2015).

93. Zhou, W. *et al.* HIF1 α induced switch from bivalent to exclusively glycolytic metabolism during ESC-to-EpiSC/hESC transition. *EMBO J.* **31**, 2103–2116 (2012).
94. Chandrasekaran, S., Li, H., Collins, J. J. & Daley, G. Q. LIN28 Regulates Stem Cell Metabolism and Conversion to Primed Pluripotency. *Cell Stem Cell* 1–15 (2016). doi:10.1016/j.stem.2016.05.009
95. He, T. L. *et al.* The c-Myc–LDHA axis positively regulates aerobic glycolysis and promotes tumor progression in pancreatic cancer. *Med. Oncol.* **32**, 1–8 (2015).
96. Hassani, S. N. *et al.* Inhibition of TGFB Signaling Promotes Ground State Pluripotency. *Stem Cell Rev. Reports* **10**, 16–30 (2014).
97. Lam, A. Q. *et al.* Rapid and efficient differentiation of human pluripotent stem cells into intermediate mesoderm that forms tubules expressing kidney proximal tubular markers. *J. Am. Soc. Nephrol.* **25**, 1211–25 (2014).
98. Hofmann, E. *et al.* Octamer-binding factor 6 (Oct-6/Pou3f1) is induced by interferon and contributes to dsRNA-mediated transcriptional responses. *BMC Cell Biol.* **11**, 61 (2010).
99. Sakaki-Yumoto, M., Liu, J., Ramalho-Santos, M., Yoshida, N. & Derynck, R. Smad2 Is essential for maintenance of the human and mouse primed pluripotent stem cell state. *J. Biol. Chem.* **288**, 18546–18560 (2013).
100. Lanner, F. & Rossant, J. The role of FGF/Erk signaling in pluripotent cells. *Development* **137**, 3351–60 (2010).
101. Jeong, W., Lee, J., Bazer, F. W., Song, G. & Kim, J. Fibroblast growth factor 4-induced migration of porcine trophectoderm cells is mediated via the AKT cell signaling pathway. *Mol. Cell. Endocrinol.* **419**, 208–216 (2016).
102. Mohammadi, M. *et al.* A tyrosine-phosphorylated carboxy-terminal peptide of the fibroblast growth factor receptor (Flg) is a binding site for the SH2 domain of phospholipase C-gamma 1. *Mol. Cell. Biol.* **11**, 5068–78 (1991).
103. Krawchuk, D., Honma-Yamanaka, N., Anani, S. & Yamanaka, Y. FGF4 is a limiting factor controlling the proportions of primitive endoderm and epiblast in the ICM of the mouse blastocyst. *Dev. Biol.* **384**, 65–71 (2013).
104. Yamanaka, Y., Lanner, F. & Rossant, J. FGF signal-dependent segregation of primitive endoderm and epiblast in the mouse blastocyst. *Development* **137**, 715–24 (2010).
105. Velling, T., Nilsson, S., Stefansson, A. & Johansson, S. β 1-Integrins induce phosphorylation of Akt on serine 473 independently of focal adhesion kinase and Src family kinases. *EMBO Rep.* **5**, 901–905 (2004).
106. Yin, X. *et al.* Synthetic RGDS peptide attenuated lipopolysaccharide/D-galactosamine-induced fulminant hepatic failure in mice. *J. Gastroenterol. Hepatol.* **29**, 1308–1315 (2014).
107. Moon, C., Han, J. R., Park, H.-J., Hah, J. S. & Kang, J. L. Synthetic RGDS peptide attenuates lipopolysaccharide-induced pulmonary inflammation by inhibiting integrin

- signaled MAP kinase pathways. *Respir. Res.* **10**, 18 (2009).
108. Guruprasad, L. *et al.* The crystal structure of the N-terminal SH3 domain of Grb2. *J. Mol. Biol.* **248**, 856–866 (1995).
 109. Egan, S. E. *et al.* Association of Sos Ras exchange protein with Grb2 is implicated in tyrosine kinase signal transduction and transformation. *Nature* **363**, 45–51 (1993).
 110. Przybyla, L., Lakins, J. N. & Weaver, V. M. Tissue Mechanics Orchestrate Wnt-Dependent Human Embryonic Stem Cell Differentiation. *Cell Stem Cell* **19**, 1–14 (2016).
 111. Wong, J. C. Y. *et al.* Definitive endoderm derived from human embryonic stem cells highly express the integrin receptors alphaV and beta5. *Cell Adh. Migr.* **4**, 39–45 (2010).
 112. Smith, a G. *et al.* Inhibition of pluripotential embryonic stem cell differentiation by purified polypeptides. *Nature* **336**, 688–690 (1988).
 113. Williams, R. L. *et al.* Myeloid leukaemia inhibitory factor maintains the developmental potential of embryonic stem cells. *Nature* **336**, 684–687 (1988).
 114. Ying, Q. L., Nichols, J., Chambers, I. & Smith, A. BMP induction of Id proteins suppresses differentiation and sustains embryonic stem cell self-renewal in collaboration with STAT3. *Cell* **115**, 281–292 (2003).
 115. Ying, Q.-L. *et al.* The ground state of embryonic stem cell self-renewal. *Nature* **453**, 519–523 (2008).
 116. Wang, L. *et al.* Akt3 is responsible for the survival and proliferation of embryonic stem cells. *Biol. Open* bio.024505 (2017). doi:10.1242/bio.024505
 117. Manning, B. & Cantley, L. AKT/PKB Signalling: Navigating Downstream. *Cell* **129**, 1261–1274 (2007).
 118. Tsuji-Tamura, K. & Ogawa, M. Inhibition of the PI3K-Akt and mTORC1 signaling pathways promotes the elongation of vascular endothelial cells. *J. Cell Sci.* **129**, 1165–1178 (2016).
 119. Hong, K.-O. *et al.* Inhibition of Akt activity induces the mesenchymal-to-epithelial reverting transition with restoring E-cadherin expression in KB and KOSCC-25B oral squamous cell carcinoma cells. *J. Exp. Clin. Cancer Res.* **28**, 28 (2009).
 120. Miner, J. H., Li, C., Mudd, J. L., Go, G. & Sutherland, A. E. Compositional and structural requirements for laminin and basement membranes during mouse embryo implantation and gastrulation. *Development* **131**, 2247–56 (2004).